

<https://doi.org/10.1038/s44182-025-00046-z>

# Soft electroadhesion systems for soft robotics

Peiwen Huang<sup>1</sup>, Yangyang Xin<sup>1,2</sup> & Pooi See Lee<sup>1,2</sup>✉

Electroadhesion (EA) offers low power consumption, material versatility, and precise force control for soft robotics. This review examines EA principles, key performance variables, and recent advances in dielectric and electrode materials. Applications such as clutches, grippers, climbing robots, and haptic interfaces are discussed. Challenges remain, including high electric field requirement and slow response. Future directions include low-voltage systems, sensing integration, advanced fabrication, and ionic-based EA technologies.

Soft robotics, characterized by using compliant materials in their structures, has emerged as a significant field in robotics research<sup>1</sup>. These robots demonstrate remarkable adaptability to environmental constraints and inherent safety in human interaction due to their material properties and structural designs<sup>2</sup>. Compared with traditional rigid robots, soft robots can perform tasks like delicate object manipulation, adaptive locomotion on various surfaces, and safe physical human-robot interaction through their compliant nature<sup>2,3</sup>. The development of reliable and versatile adhesion and gripping technologies is crucial for advancing soft robotics capabilities<sup>2</sup>. This is particularly important for applications such as handling fragile objects, climbing on various surfaces, navigation of complex terrains or haptic interactions.

Conventional methods for adhesion and gripping each have their own limitations<sup>4</sup>. Mechanical grippers can damage delicate objects and struggle with small or thin materials. Magnetic adhesion is only effective on ferromagnetic materials. Vacuum suction requires continuous power consumption, is not suitable for porous surfaces, and cannot operate in vacuum environments. Van der Waals adhesion offers limited force and lacks efficient reversibility control mechanisms. A concise comparison of these conventional adhesion methods is provided in Table 1, highlighting their respective advantages and drawbacks.

Electroadhesion (EA) represents an emerging adhesion technology that operates through electrostatic attraction, where adhesion and release can be controlled by potential difference<sup>5</sup>. The fundamental structure of EA devices consists of a pair of electrodes, typically arranged in an interdigital (interdigitated) configuration, encased within a dielectric film<sup>6,7</sup>. When an EA device is positioned on a substrate and high voltage is applied, the resulting non-uniform electric field induces either polarization or charge redistribution on the substrate surface, depending on its electrical properties, which will both generate electrostatic forces between the substrate and the electrodes<sup>6,8</sup>.

One of the key advantages of EA lies in its versatility and adaptability compared to other adhesion mechanisms<sup>9</sup>. EA systems can effectively

generate adhesion forces on a broad spectrum of surface types, ranging from electrically conductive to insulating materials<sup>7</sup>. Another crucial feature of EA technology is its controllability - the adhesion force can be modulated by adjusting the applied voltage and completely dissipates upon voltage removal<sup>10</sup>. This technology reduces system complexity through its lightweight construction and simple structure<sup>4,5,9</sup>. Furthermore, EA systems offer significant energy efficiency advantages - while requiring high voltage for operation, power consumption remains remarkably low due to minimal current flow (usually several  $\mu\text{A}$ ) during steady-state operation<sup>5</sup>. Reported EA devices span a wide power range depending on application and scale. For instance, one study on a wearable exoskeleton clutch reported power consumption as low as  $\sim 0.6 \text{ mW}$ <sup>11</sup>; another EA clutch for mobile robots recorded  $\sim 0.3 \text{ W}$ <sup>12</sup>; and a suction-based EA gripping system in a separate work reached up to  $\sim 1.5 \text{ W}$ <sup>13</sup>. EA also enables gentle material handling through soft EA pads, allowing it to lift delicate and high-value objects<sup>14</sup>. Additionally, EA can potentially operate in extreme environments such as vacuum conditions, making it particularly promising for space applications<sup>5</sup>. Table 2 summarizes typical parameter ranges for EA devices, including dielectric thickness, operating voltage, and corresponding adhesion forces, serving as a practical reference for device design and performance assessment.

Recent developments in soft robotics have witnessed increasing integration of EA technology, where flexibility, adaptability, and gentle manipulation capabilities are essential requirements<sup>14,15</sup>. Advances in flexible electrode design and dielectric material selection have substantially enhanced EA system performance in dynamic applications<sup>16–18</sup>. In soft robotic grippers, EA enables precise manipulation of fragile objects and thin sheets through controllable adhesion forces and largely increase the payload of the soft gripper<sup>14,15,19</sup>. In clutch applications, EA provides electrically controllable braking and attachment capabilities with low power consumption<sup>20</sup>. For robotic locomotion, EA facilitates stable adhesion at specific points for resting and controlled movement across surfaces<sup>21,22</sup>. In

<sup>1</sup>School of Materials Science and Engineering, Nanyang Technological University, 50 Nanyang Avenue, Singapore, Singapore. <sup>2</sup>Singapore-HUJ Alliance for Research and Enterprise (SHARE), Smart Grippers for Soft Robotics (SGSR)/Campus for Research Excellence and Technological Enterprise (CREATE), Singapore, Singapore. ✉e-mail: [pslee@ntu.edu.sg](mailto:pslee@ntu.edu.sg)

Table 1 | Comparison of different adhesion technology

Method	Principle	Advantages	Limitations	Uses
Chemical Adhesive <sup>126,127</sup>	Bonds to surfaces via chemical/physical reactions	High bonding strength; mature technology; relatively low cost	Often single-use; can leave residues; sensitive to temperature/humidity	Structural bonding; electronics assembly
Vacuum Suction <sup>128-130</sup>	Negative pressure in a sealed cup	Strong grip on flat parts; well-established industrial use	Requires continuous pumping; poor on porous/uneven surfaces; not for vacuum env.	Automated handling; factories (e.g., sheets, panels)
Magnetic <sup>31,132</sup>	Magnet fields acting on ferromagnetic objects	Simple design; robust with metal objects	Only for ferrous materials, may magnetize workpieces	Transferring steel/iron parts; machining lines
Van der Waals/Gecko <sup>133</sup>	Relies on intermolecular forces or micro/nanofiber structures	Adheres to most materials; reusable; can be cleaned	Expensive fabrication; needs relatively clean/smooth surfaces; lack of or difficulty in reversibility control	Delicate parts; bio-inspired climbing robots
Electroadhesion (EA) <sup>4,5</sup>	High voltage electrodes generating electrostatic forces	Works on various surfaces; very low power; leaves minimal residue	Requires high voltage; sensitive to humidity/roughness; moderate force on rough	Robotic grippers; wall-climbing robots; semiconductor handling

Table 2 | Typical Parameter Ranges for EA Devices

Parameter	Typical Range
Dielectric Layer Thickness	Submicrometer (<1 μm) up to a few millimeters
Operating Voltage	~0.04 kV up to ~9–10 kV
Power Consumption	Typically from below 1 milliwatt (mW) to several watts (W)
Adhesion Force	Fractions of newtons to tens of newtons

human-machine interfaces, EA-based haptic devices create controllable tactile sensations through modulated friction forces<sup>23,24</sup>. These capabilities have significantly expanded the potential applications of EA in soft robotics, establishing it as a crucial technology for next-generation robotic systems.

This review aims to explore the fundamental principles underlying EA technology, with particular focus on materials selection and fabrication methodologies. We will investigate various applications of EA in soft robotics. Additionally, we will discuss current technological challenges in EA implementation and propose research directions aimed at overcoming these limitations. Through this comprehensive analysis, we aim to provide insights into both the current state and prospects of EA technology in soft robotics.

Principles of Electroadhesion and Influential Variables

EA depends on electrostatic forces between electrodes and a surface to generate adhesion. As depicted in Fig. 1a, when a voltage is applied across the electrodes of an EA pad, it creates an electric field. For dielectric materials, this field polarizes the object’s surface, inducing dipole moments that result in attractive forces between the EA pad and the object. For conductive materials, the electric field prompts charge redistribution on the surface rather than polarization, yet it similarly produces an adhesion force<sup>5</sup>. As studies on EA have evolved, several theoretical models have been adopted to describe and predict these forces including models based on Coulomb forces and Johnsen-Rahbek (J–R) effect.

From a microscopic perspective, EA is based on Coulomb forces between charges. For continuous charge distributions and fields, this microscopic mechanism is elegantly represented by the Maxwell stress tensor - a macroscopic description that can be derived from Coulomb’s law through field theory. This tensor describes the stress generated by an electric field in a dielectric medium and provides a more practical way to calculate the forces in real applications<sup>25-27</sup>. The Maxwell stress tensor in its general form is expressed as:

$$T_{ij} = \epsilon \left( E_i E_j - \frac{1}{2} \delta_{ij} E^2 \right)$$

(1)

Where  $\epsilon$  is the dielectric constant,  $E_i$  and  $E_j$  are the components of the electric field, and  $\delta_{ij}$  is the Kronecker delta. This equation helps calculate the stress at any given point in the material, resulting from the interaction of electric field components.

This tensor equation describes the complete stress state at any point in the dielectric medium. For the specific case of a parallel electrode configuration, where the electric field is predominantly normal to the electrode surface and uniform across the interface, the tensor equation can be simplified. By integrating the normal component of the stress over the electrode area, we obtain a more practical expression for the total EA force<sup>28</sup>:

$$F = \frac{A}{2} \epsilon_0 \left( \frac{k_d V}{d} \right)^2$$

(2)

where A is the contact area between the electrodes, V is the applied voltage, d is the thickness of the dielectric layer,  $\epsilon_0$  is the permittivity of free space and  $k_d$  is the dielectric constant of the dielectric layer. In this model, the dielectric material is considered as an ideal insulator and the air gap is ignored in this model.

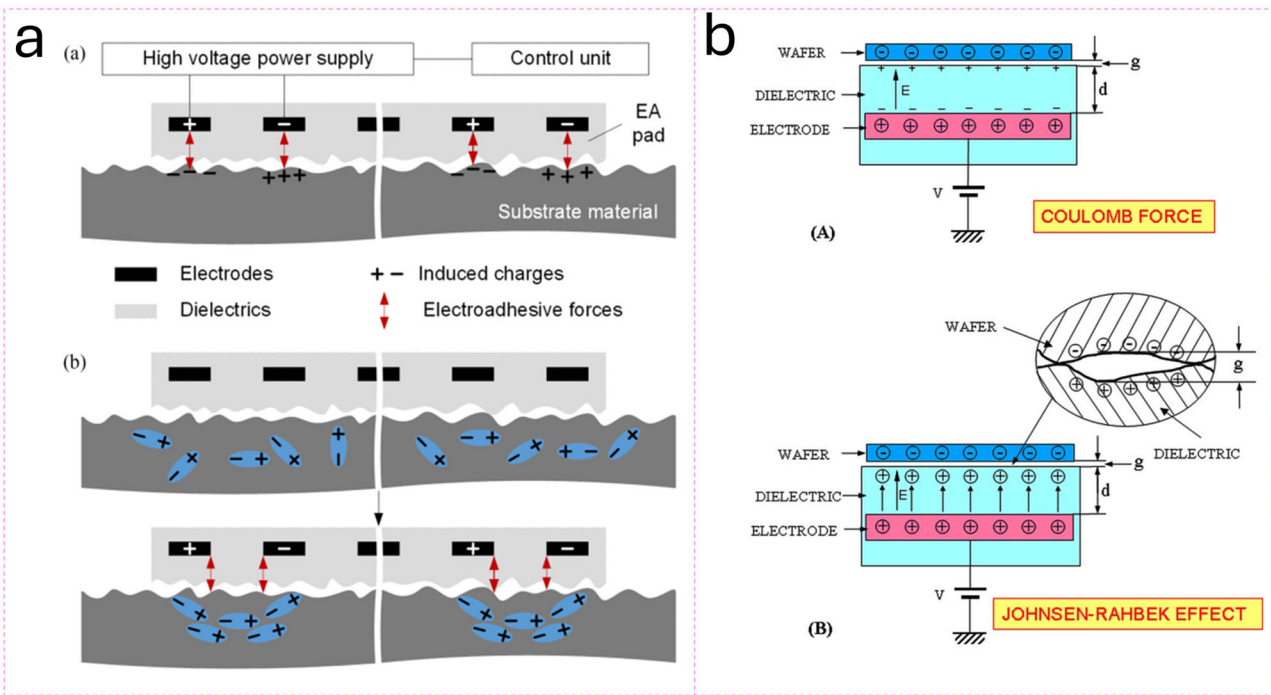


**Fig. 1 | Working principle of the EA.** **a** Schematic illustration of working principles for an EA system working on conductive and dielectric substrate in cross-sectional view. Reproduced under the Creative Commons Attribution 4.0 International License (CC BY 4.0)<sup>5</sup>. Copyright 2019 IEEE. **b** Schematic illustration of two

electrostatic clamping mechanisms: classical/conventional electrostatic model and Johnson-Rahbek electrostatic model. Reproduced with permission<sup>28</sup>. Copyright 2007 AIP Publishing LLC.

The Johnson–Rahbek (J–R) effect, which occurs when charge carriers are able to transit through the dielectric layer, also initiates EA, as shown in Fig. 1b. This process involves the flow of current through conductive materials such as polyelectrolytes or semiconductors, which facilitates the migration of charges to the surface areas of the dielectric films. An electric field is established across a nanometer-scale gap, either between juxtaposed dielectric layers or between a dielectric layer and an adjacent electrode. The resulting attractive force due to the J–R effect can be expressed as<sup>28</sup>:

$$F_{JR} = \frac{A_{real}}{2} \epsilon_0 \left( \frac{k_g V_{eff}}{g} \right)^2 \quad (3)$$

where  $A_{real}$  is the real contact area between the nanoscale asperities on the surfaces,  $g$  is the size of the interfacial gap,  $k_g$  is the relative permittivity of the interfacial gap and  $V_{eff}$  is the effective applied voltage, which is affected by the resistances of the dielectric material and the contact interface.

Maxwell adhesion force and J–R effect typically coexist in EA systems, but their relative contributions vary depending on the material properties. Maxwell stress becomes dominant when the electrodes are encapsulated in highly insulating dielectric layers, which is common in EA devices designed for grippers or locomotion robots that need to work with various substrate materials. Conversely, the J–R effect becomes predominant when the dielectric layer has higher conductivity. The J–R effect can generate larger electrostatic pressures at a given voltage because the charge carriers migrate to the dielectric-electrode interface, leading to a substantial reduction in the interfacial air gap ( $g$ ), which is typically much smaller than the thickness of the dielectric film. Therefore, J–R-dominated systems are more suitable for applications requiring large adhesion forces but limited to specific materials and interfaces, such as EA chucks or clutches.

Originally, it was believed that the effectiveness of adhesion was determined by a few key factors: the dielectric constant and thickness of the dielectric layer, the applied voltage, and the surface texture. However, recent developments have identified as many as 33 different variables that can

influence adhesion<sup>29</sup>, complicating its management without sacrificing certain properties to meet specific requirements.

While Maxwell and J–R effect models can effectively evaluate the EA force in parallel-plate electrode configurations, these models face significant limitations when applied to interdigital electrode designs. The challenges arise from two main aspects: first, the complex electrode patterns generate inhomogeneous electric field distributions that are difficult to model accurately; second, the diverse working mechanisms and material properties of different substrates introduce additional variables. Consequently, developing a universal model to predict EA performance remains challenging. Nevertheless, ongoing research continues to investigate both qualitative and quantitative relationships between various parameters and EA device performance. Recent researchers have increasingly adopted Finite Element Method (FEM) simulation to predict EA device performance, as it can better account for the complex field distributions and geometric effects<sup>30</sup>.

Among the numerous variables that influence EA performance, the following aspects have been identified as particularly important and have received substantial research attention.

### Electric field

The theoretical models of Maxwell stress and Johnson-Rahbeck effect both predict that the electrostatic adhesion force should increase quadratically with applied voltage, which was initially supported by early experimental results. However, subsequent experimental studies revealed significant deviations from this quadratic relationship at higher voltage ranges. These deviations are primarily attributed to two phenomena: dielectric breakdown and field emission effects. The dielectric breakdown leads to a dramatic increase of the leaking current when the electric field reaches the material's breakdown strength, while field emission becomes prominent at high field intensities, particularly at surface irregularities and sharp edges.

This non-linear behavior was first systematically documented by Stuckes et al., who demonstrated that beyond a critical threshold voltage, the force-voltage relationship deviates substantially from the quadratic prediction<sup>31,32</sup>. Their findings highlighted the importance of considering

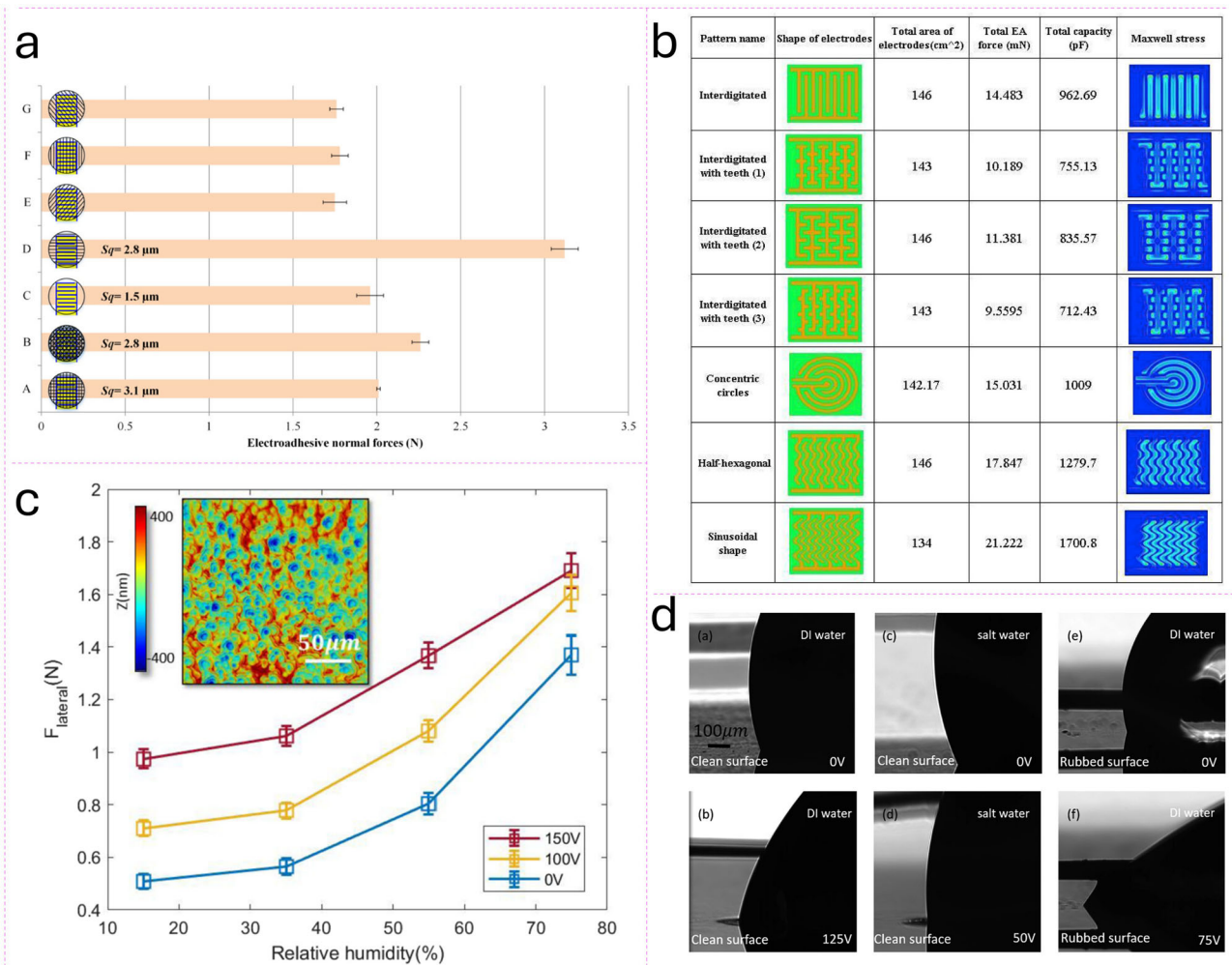


**Fig. 2 | Study of some influential variables of EA system.** **a** EA force on aluminum with different textures. Reproduced under the Creative Commons Attribution 3.0 License (CC BY 3.0)<sup>29</sup>. Copyright 2016 IOP Publishing Ltd. **b** Simulation results of performance of EA device with different electrode patterns. Reproduced with

permission<sup>30</sup>. Copyright 2021 Elsevier B.V. **c** Configuration of the finger-EA interface mechanism of a haptic device with EA. Reproduced with permission<sup>45</sup>. Copyright 2020 IEEE. **d** Electrowetting effect. Reproduced with permission<sup>45</sup>. Copyright 2020 IEEE.

these high-field effects in practical applications. Building upon this work, Atkinson et al. developed a more comprehensive model that incorporated additional factors previously overlooked<sup>33</sup>. His revised formula for the adhesion force is:

$$\frac{F}{A} = \frac{V_i^2}{88.8 \times 10^{11} d_{\max}^2} \left( 1 + 2 \ln \left( \frac{V_{\max}}{V_i} \right) \right) \quad (4)$$

Where  $F$  represents the adhesion force,  $A$  is the contact area,  $V_i$  is the interfacial voltage drop,  $d_{\max}$  is the maximum height of the surface asperity, and  $V_{\max}$  is the interfacial potential corresponding to the advent of field emission across the entire interface. The interfacial voltage drop is a critical parameter that significantly differs from the total applied voltage due to the distribution of electrical resistance in the system, especially at the microscopic contact points between the two materials. This drop mainly occurs at the interface between the metal electrode and the semiconductive dielectric, where microscopic surface roughness results in a small actual contact area and high local resistance.

### Surface roughness

In addition to the applied electric field, surface texture significantly influences EA performance through its effect on interfacial contact characteristics<sup>34</sup>. Surface roughness, characterized by microscopic peaks and

valleys, reduces the effective contact area between the electrode and the target surface<sup>35,36</sup>. This reduction occurs because air gaps form at the interface, and since the dielectric constant of air is substantially lower than that of most solid dielectric materials, these gaps significantly diminish the regions where the electric field can effectively generate EA force. Consequently, increased surface roughness typically results in reduced adhesive force. Conversely, smoother surfaces facilitate larger real contact areas due to more intimate contact between the substrate and the EA device. This enhanced interfacial contact promotes more uniform electric field distribution across the interface, leading to stronger adhesion forces<sup>36</sup>.

Experimental validation of these effects has been provided through several systematic studies. The study of Ruffatto et al. compared the performance of different adhesion methods across surfaces with varying roughness, including EA<sup>37</sup>. Their results demonstrate that EA exhibits optimal performance on relatively smooth surfaces (roughness < 10 μm), with adhesion forces decreasing substantially on rougher surfaces. These findings were further corroborated by Guo et al. who performed a comprehensive investigation of the relationship between surface texture and interfacial EA force (Fig. 2a)<sup>29</sup>. Their study revealed two critical thresholds: surfaces with root mean square roughness ( $S_q$ ) below 2 μm showed minimal impact on EA force, while those exceeding 5 μm demonstrated significant force reduction. Furthermore, their research highlighted that the directional characteristics of surface texture (texture orientation) can also modulate the



EA force, suggesting that both amplitude and spatial distribution of surface features play important roles in determining adhesion strength.

### Electrode pattern

The electrode pattern design significantly influences EA performance. Experimental studies have demonstrated that optimized electrode configurations within EA pads of the same size can enhance the adhesion force by up to 15 times compared to non-optimized designs<sup>7</sup>. The most widely adopted pattern is interdigital, owing to its ability to generate hemispherical equipotential fields at the interface between electrode pairs. The polarization of the substrate surface is predominantly determined by the electric field distribution between positive and negative electrodes, suggesting that interdigital structures with optimized electrode gaps can achieve superior performance. To maximize the adhesion force while ensuring operational stability, the electrode gap is typically minimized within the constraints of dielectric breakdown strength of the insulating materials<sup>38</sup>.

While most earlier research on optimizing electrode patterns primarily relied on experimental results<sup>6,39,40</sup>, recent years have seen a growing use of finite element method (FEM) simulations. These simulations are used to compare different electrode configurations and aid in the design of EA pads<sup>6,30,41–43</sup>. Choi et al. explored the impact of electrode geometry on local charge distribution and interface polarization. They constructed devices with varying electrode gaps and widths and analyzed the force under different voltages. Their results indicate that the EA force increases with decreasing electrode gap and width. This effect arises because, for a given device area, a smaller electrode gap and width lead to a larger electrode boundary edge ratio, which is crucial for EA on insulating or dielectric materials<sup>38</sup>. Bigharaz et al. utilized ANSYS Maxwell, an FEM-based software, to evaluate the 2D and 3D electrodes, arriving at a similar conclusion that smaller electrode widths enhance capacitance and adhesion performance. Additionally, innovative patterns such as sinusoidal have been shown to possess higher capacitance compared to the common interdigitated pattern, as shown in Fig. 2b<sup>30</sup>. Ruffatto et al. compared different electrode shapes through simulation and experiments, concluding that concentric designs perform better due to their larger and more evenly distributed electric fields<sup>44</sup>.

### Environmental factors

Environmental factors significantly influence the performance and reliability of EA devices. Among these factors, humidity and temperature have been identified as particularly critical through both theoretical analysis and experimental studies.

Humidity affects EA through multiple mechanisms and these effects are most extensively studied in EA haptic devices, where humidity variations come from both environmental moisture and human perspiration as depicted in Fig. 2c<sup>23,45–47</sup>. When water molecules accumulate at the interface between the EA device and substrate, they form capillary bridges that alter the local electric field distribution. The presence of water reduces the EA force through two primary mechanisms: (1) creating conductive paths that drastically reduce the interface impedance, and (2) bridging the air gaps between the finger and touchscreen surface, which diminishes the potential difference across the interface. These effects result in reduced electric field strength and consequently weakened EA forces<sup>48</sup>. However, in haptic applications, studies have shown that increasing humidity can enhance the EA-induced friction force within certain ranges. This enhancement is attributed to multiple factors including decreased Young's modulus of skin leading to larger contact area, increased capillary force, and the electro-wetting effect as shown in Fig. 2d. Notably, electrowetting has been found to contribute up to 60% of the total friction force increase in some cases<sup>45</sup>. Based on these observations, potential strategies to address the humidity effects could include the use of hydrophobic surface treatments, moisture-resistant dielectric materials, or optimized surface structures.

Another critical environmental factor is temperature<sup>49</sup>. Elevated temperatures generally deteriorate EA device performance through multiple mechanisms: reducing material resistivity, altering dielectric constants, and

potentially causing thermal expansion that affects the contact interface. These combined effects typically result in reduced adhesion forces and increased leakage current<sup>18</sup>. Interestingly, recent research by Choi et al. has revealed an unexpected benefit of higher temperatures: improved tactile feedback for users due to an enhanced ratio between base friction and EA-induced additional friction, which could be particularly beneficial in human-machine interface applications<sup>50</sup>. This finding suggests the potential for optimizing temperature effects based on specific application requirements rather than viewing thermal effects as purely detrimental.

## Dielectric and electrode materials for electroadhesion

### Dielectric materials and their fabrication

A wide range of dielectric materials can be employed in EA devices. While theoretically any dielectric material could function, the performance of an EA device is critically dependent on the specific properties of the chosen material<sup>4</sup>. According to the Maxwell stress equation, the generated Maxwell stress is proportional to the material's dielectric constant. Moreover, since electrical breakdown can occur both between electrodes and within the dielectric film itself, the breakdown strength of the dielectric material determines the maximum applicable voltage, thereby directly influencing the maximum achievable EA force. Beyond these electrical properties, mechanical characteristics such as compliance become particularly crucial when considering materials for soft robotics applications.

To enhance clarity and cohesion, representative dielectric materials are described in terms of their key properties (Table 3)—namely, dielectric constant, breakdown strength, stretchability, and mechanical characteristics—as each material naturally exhibits different combinations of these traits, which significantly influence EA performance in various application scenarios. For example, polyimide (PI) films, though less stretchable, are prized for their high dielectric strength and stability, making them suitable for high-voltage applications or environments. Poly(vinylidene fluoride) (PVDF) and its copolymers combine relatively high dielectric constants with moderate flexibility; they can be further enhanced by incorporating ceramic or conductive nanofillers, which is advantageous for EA devices requiring higher force densities. In contrast, silicone-based elastomers (e.g., PDMS, Ecoflex) offer exceptional stretchability and compliance, thus improving conformity to rough or curved surfaces but often exhibit lower dielectric constants. Lastly, other soft elastomers such as polyurethane (PU) or commercial Very High Bond (VHB) tapes can bridge the gap by providing decent dielectric strength, moderate stretchability, and, in some cases, extra functionalities like self-healing. Through careful matching of their electrical and mechanical properties with the target EA application—whether it demands extreme shape adaptation, high normal force—one can optimize both the adhesion performance and overall reliability of the EA system.

For soft robotics applications, flexible materials are generally preferred. Polyimide (PI) stands out among flexible dielectric materials due to its exceptional combination of mechanical properties, environmental stability, and high dielectric breakdown strength<sup>17,19,25,51,52</sup>. Commercial PI films are available with precisely controlled, uniform thicknesses, making them ideal for direct use as dielectric layers without additional processing requirements. The superior mechanical and dielectric strength of PI enables the fabrication of dielectric layers as thin as 25  $\mu\text{m}$  while maintaining reliable operation under high electric fields. This characteristic allows PI-based EA devices to generate substantial adhesion forces. In practical applications, PI-based EA devices have demonstrated remarkable success in soft robotics, particularly in locomotion robots developed by Gu et al. and Guo et al. These devices generated sufficient adhesion force to not only support the entire robot weight on flat surfaces but also enable stable locomotion across varying substrates (Fig. 3a)<sup>53,54</sup>. A limitation of PI is its relatively low flexibility compared to other elastomeric materials, which can limit its performance in highly flexible or stretchable applications. Despite this, its exceptional dielectric properties and mechanical strength make it a preferred choice for high-force applications. In a comprehensive comparative study by Hwang et al., PI-based EA devices showed superior performance

Table 3 | Summary of Representative Dielectric Materials for EA Applications

Material	Dielectric Constant	Breakdown Strength	Mechanical Properties	Advantages	Limitations
Polyimide (PI) <sup>51,134,135</sup>	3.4–3.5	High (> 200 kV/mm)	Flexible, high modulus, limited stretchability	Excellent dielectric strength, commercial availability with controlled thickness	Limited stretchability
PVDF <sup>20,57,136</sup>	8–11 (base), >50 (composites)	Moderate to high	Flexible, moderate stiffness	High dielectric constant, tunable properties	Complex processing
Silicone elastomers (PDMS, Ecoflex) <sup>137</sup>	2.5–3.0	Moderate	Highly stretchable, low modulus	Excellent stretchability, commercial availability	Low dielectric constant
Polyurethane (PU) <sup>65,138</sup>	3.0–7.0	Moderate	Tunable mechanical properties	Highly tunable properties, potential for self-healing	Complex synthesis, lower stability

compared to PDMS and acrylic elastomers in gripper applications<sup>51</sup>. Their high modulus prevented unintentional deformation during object manipulation, effectively providing structural reinforcement. Their large-area PI-based EA gripper successfully manipulated objects weighing over 16.8 kg, as depicted in Fig. 3b. Another limitation of using commercially available PI films, compared to self-fabricated dielectric films, is the reduced flexibility in tuning mechanical and dielectric properties such as thickness or dielectric strength.

Polyvinylidene fluoride (PVDF) represents another significant class of flexible dielectric materials, distinguished by its excellent flexibility and inherently high dielectric constant<sup>55,56</sup>. Research efforts have focused on enhancing PVDF-based materials to achieve even higher dielectric constants, particularly crucial for applications demanding substantial forces, such as EA clutches and tapes. Wei et al. developed an innovative approach to fabricating PVDF-based dielectric nanocomposites with ultrahigh dielectric constants while maintaining breakdown strength<sup>20</sup>. By incorporating Ti<sub>3</sub>C<sub>2</sub>T<sub>x</sub> into a terpolymer P(VDF-TrFE-CTFE), nanocomposite films with a dielectric constant exceeding 2300 at 100 °C were produced. A clutch using this nanocomposite achieved an EA shear stress of 85.61 N/cm<sup>2</sup> at 500 V and 70 °C. Similarly, as shown in Fig. 3c, Ranjithkumar et al. added hexagonal Boron Nitride (hBN) and BaTiO<sub>3</sub> into a PVDF-HFP matrix, allowing the device to operate at a lower voltage of 250 V and increasing the payload from 100 g to 950 g<sup>57</sup>. The preparation method for PVDF-based films involves mechanically mixing PVDF with other components in a solution, coating the mixture onto a substrate, and then evaporating the solvent to solidify the film. This method is relatively simple and adaptable, making it suitable for small-scale research and capable of easily fabricating microscale films with good uniformity. However, it may encounter issues with solvent evaporation, potentially leading to uneven film thickness or surface irregularities. While the method is cost-effective in terms of equipment, the use of high-quality solvents and additional processing steps may increase production costs, particularly for large-scale applications.

While flexible dielectric materials excel in applications requiring minimal deformation, such as crawling robot feet or EA clutches operating on relatively flat or cylindrical surfaces, applications demanding higher compliance necessitate the use of stretchable dielectric materials, particularly dielectric elastomers. Although these stretchable materials typically exhibit lower dielectric strengths, they offer superior conformability to complex surface geometries, effectively minimizing air gap formation and accommodating surface irregularities. This enhanced surface adaptation results in larger and more stable EA forces, ultimately improving overall performance<sup>58</sup>. Furthermore, the integration of EA devices with soft actuators often benefits from using similar or identical materials, as many soft actuators are inherently constructed from stretchable materials.

Among stretchable dielectric materials, silicone-based elastomers have gained widespread adoption due to their commercial availability, exceptional mechanical properties, high dielectric strength, and remarkable stretchability. The Ecoflex series and polydimethylsiloxane (PDMS) are particularly prominent choices, as depicted in Fig. 3d. These materials are typically prepared by directly using commercially available precursors, which are mixed and then processed into thin films through coating methods, usually employing the doctor blade technique. The films are subsequently thermally cured to achieve a solid state. This fabrication approach is cost-effective and convenient, but it may have limitations in terms of uniformity and precise control over the film thickness. Guo et al. demonstrated the effectiveness of this approach by embedding an EA device within a pneumatic two-finger gripper fabricated from Ecoflex 00-50<sup>15</sup>. This allowed the gripper to handle thin, flat objects like plastic PVC ID cards, porous cotton-polyester fabric, and CDs, which are typically difficult for conventional pneumatic grippers to manage. Shintake integrated EA technology with dielectric elastomer actuators (DEA) to develop an electrically controlled soft gripper<sup>14</sup>. In this system, PDMS served both as the dielectric layer for the EA device and the passive layer for the DEA, enabling the gripper to perform bending motions. Leveraging PDMS's high modulus, the gripper successfully handled a variety of objects, including delicate items

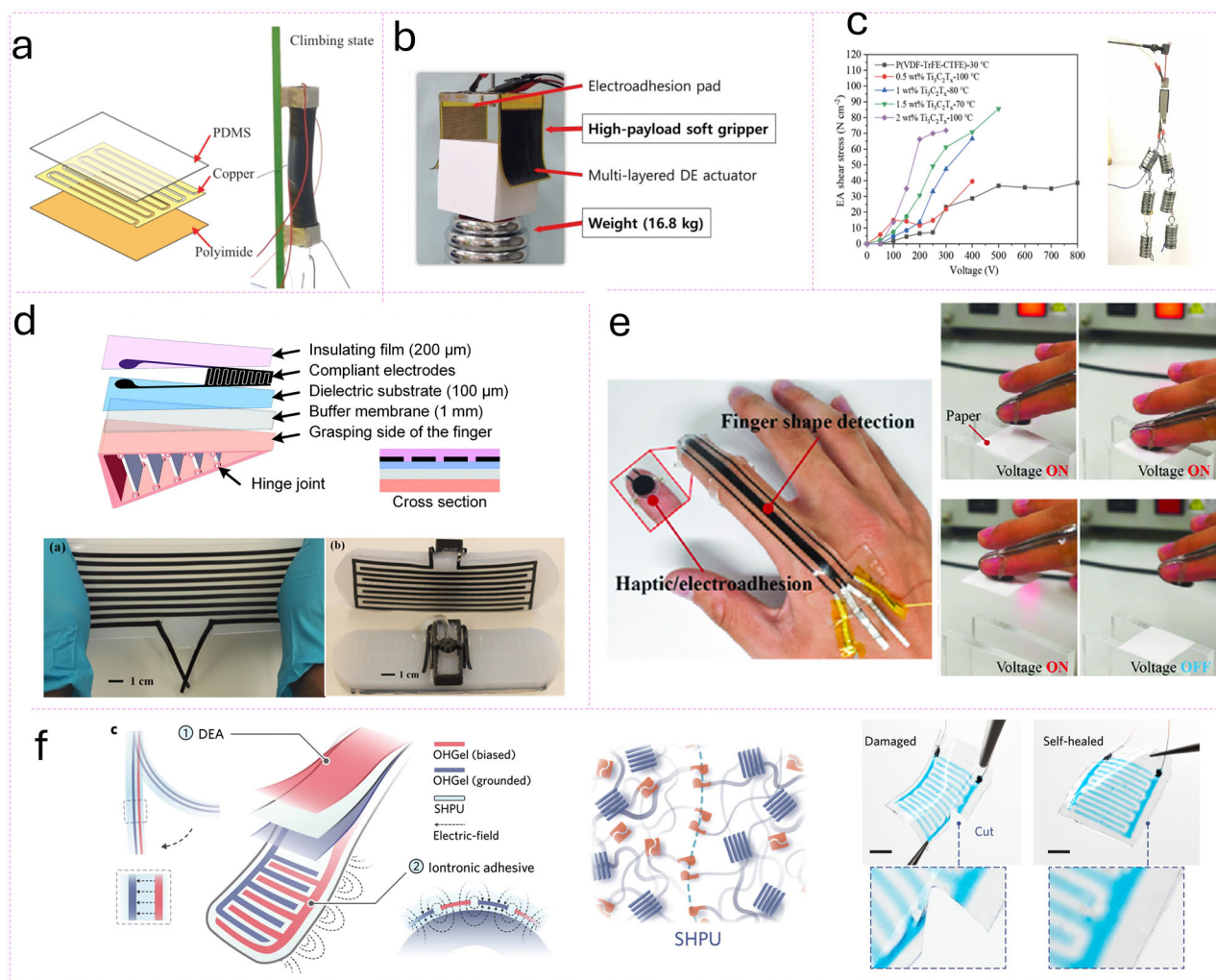


**Fig. 3 | Dielectric materials for soft EA device.** **a** PI-based EA device for a climbing robot. Reproduced with permission<sup>54</sup>. Copyright 2022 Elsevier B.V. **b** Comparison of PI with other common dielectric materials, and high-payload electroadhesive gripper utilizing PI as the dielectric layer. Reproduced with permission<sup>51</sup>. Copyright 2021 IEEE. **c** Schematic illustration of the fabrication process for a high-dielectric-constant PVDF-based composite material and an EA clutch utilizing another PVDF-based dielectric material. Reproduced with permission<sup>20,57</sup>. Copyright 2023 Mary Ann Liebert, Inc. Copyright 2023 Springer Nature. **d** Silicone as the dielectric layer of

EA devices for soft robotic grippers. Reproduced with permission<sup>59</sup>. Copyright 2019 Mary Ann Liebert, Inc. Reproduced under the Creative Commons Attribution 3.0 License (CC BY 3.0)<sup>15</sup>. Copyright 2018 IOP Publishing Ltd. **e** A wearable EA device with VHB as the dielectric material. Reproduced under the Creative Commons Attribution 4.0 International License (CC BY 4.0)<sup>63</sup>. Copyright 2020 The Authors. Published by Wiley-VCH GmbH. **f** The schematic demonstration of a PU-based EA gripper and its self-healing capability. Reproduced under the Creative Commons Attribution 4.0 International License (CC BY 4.0)<sup>65</sup>. Copyright The Author(s) 2023.

like raw chicken eggs, flat sheets of paper, and fragile water balloons—tasks that would have been impossible for a DEA-only gripper due to its limited gripping force. Chen et al. also used a PDMS-based EA device in an Ecoflex soft gripper, achieving a normal adhesion force of up to 4.11 kPa and a shear force of 12.78 kPa<sup>59</sup>. This enhancement not only increased the gripper's maximum payload but also improved its ability to grasp thin and flat objects, expanding the maximum lifting sphere diameter from 250 mm to 300 mm.

VHB (Very High Bond) is another highly popular, commercially available dielectric elastomer film. Since VHB is commercially available and can be used directly without the need for further processing, it provides significant convenience in various applications. However, this also means that its material properties cannot be adjusted, and the thickness options are limited. It is widely used as the dielectric layer in dielectric elastomer actuators (DEAs) due to its excellent dielectric properties and stretchability<sup>60,61</sup>. VHB is a promising option as the dielectric layer in EA systems because it offers both the high dielectric constant and dielectric strength required for EA devices. Additionally, since DEAs are often coupled with EA devices due to their similar working mechanisms, using VHB for both components can simplify

fabrication<sup>62</sup>. As shown in Fig. 3e, Kanno et al. successfully demonstrated this versatility by implementing VHB as the dielectric layer in a wearable EA device, where its excellent stretchability enabled seamless conformity to finger movements<sup>63</sup>. Their device not only provided reliable adhesion under DC voltage but also delivered haptic feedback through AC voltage activation, highlighting the multifunctional capabilities of the EA system.

Polyurethane (PU) emerges as a particularly versatile option among dielectric elastomers, distinguished by its higher dielectric constant compared to silicone materials. Unlike commercially available silicone elastomers and VHB tape, PU-based materials offer unprecedented tunability in their properties. Through modifications in chemical composition and processing methods, key characteristics such as hardness, elastic modulus, and dielectric strength can be precisely controlled. Moreover, novel functionalities including self-healing and self-cleaning capabilities can be engineered into the material. Choi et al. used an anionic waterborne polyurethane (WPU) as the dielectric material for an EA gripper, achieving a maximum force of 33.1 kPa under a voltage of 1 kV<sup>64</sup>. Gao et al. developed a supramolecular, hierarchically H-bonded polyurethane (SHPU) as the



dielectric layer for an EA gripper, which not only enhanced mechanical toughness but also imparted self-healing properties to the device (Fig. 3f)<sup>65</sup>. Their innovation enabled the EA device to recover functionality even after severe mechanical damage, demonstrating unprecedented resilience in practical applications. Compared to commercial materials, synthesized PU may involve more complex fabrication processes and exhibit lower stability. Additionally, since PU typically has undesirable properties such as lower dielectric strength and higher viscosity, modifying PU materials is crucial for enhancing device performance.

In addition to each material's intrinsic properties, the method of fabricating the dielectric layer strongly impacts the reliability and overall EA performance. For instance, when using commercially supplied PI or VHB tapes, the film thickness and modulus are fixed; researchers typically laminate or bond these thin sheets onto patterned electrodes. By contrast, when self-fabricating elastomeric layers such as silicone or PU, one may employ casting, blade-coating, or spin-coating. Each of these methods can produce uniform films but differs in thickness range, scalability, and substrate compatibility. Casting more easily handles thicker layers, blade-coating is quick and adaptable to larger areas, while spin-coating can yield very thin and uniform films but typically suits smaller substrates.

For materials like PVDF, which are often dissolved in a solvent before curing, the film can be cast or spin-coated to reach the desired thickness. Proper solvent evaporation and annealing steps are crucial to ensure consistent crystallinity and electrical performance. If fillers (e.g., ceramic or carbon-based) are added, thorough dispersion (via sonication, ball milling, etc.) is necessary before coating to avoid aggregation.

More compliant elastomers can conform to irregular surfaces, reducing air gaps. Balancing dielectric strength, thickness, elasticity, and ease of fabrication is essential when selecting or formulating a dielectric for EA systems, especially for soft robotic applications.

### Electrode materials and their fabrication

The performance of EA devices critically depends on patterned electrodes that generate the desired electric field distribution. Common electrode materials include metals and carbon-based materials (such as carbon black, CNTs, graphene, and their composites), each offering distinct advantages for specific applications. Metal electrodes are traditionally preferred due to their superior conductivity and compatibility with diverse fabrication methods that enable precise patterning—a crucial requirement for optimizing EA performance. While metal films can be directly cut into free-standing interdigitated patterns and applied to dielectric films, offering excellent conductivity and pattern uniformity<sup>54</sup>, this approach has limitations. Conventional free-standing metal films often prove too thick and lack the flexibility required for many applications. Consequently, direct deposition of thin metal layers onto flexible dielectric substrates has emerged as a more effective approach, as these thinner layers can better accommodate substrate deformation<sup>19,38,53</sup>. Hwang et al. conducted comprehensive comparisons of various electrode materials in EA devices, demonstrating that 17  $\mu\text{m}$  gold electrodes outperformed both silver nanowire (AgNW) and carbon nanotube (CNT) electrodes, primarily due to their more uniform pattern structure compared to the network-like arrangements typical of 1D materials<sup>51</sup>. Similarly, Gu et al. successfully implemented 18  $\mu\text{m}$  copper patterns on PI substrates to create EA feet for climbing robots, achieving sufficient adhesion force to support vertical locomotion<sup>53</sup>. However, even these thin metal layers face significant challenges including potential delamination from the substrate during repeated deformation cycles, susceptibility to fatigue cracking under mechanical stress, and limited stretchability that may constrain their application in highly deformable EA devices.

To address the time-consuming nature of traditional metal electrode patterning, commercial conductive inks—typically consisting of metal particles (predominantly silver) dispersed in appropriate solvents—have gained popularity due to their processing advantages. These inks are compatible with conventional printing methods such as blade coating and screen printing. For example, Wang et al. used screen printing to apply silver paste

onto PI film for a climbing robot<sup>21</sup>. The PI film served as the belt for the crawler. The stable performance of the rotating EA belt highlights the robust adhesion of the printed silver electrodes to the PI substrate, ensuring they remain intact during operation, while also preserving the device's overall flexibility. Beyond traditional methods, these conductive inks enable the use of advanced manufacturing techniques like inkjet printing, which offers superior resolution for creating precise patterns with minimized electrode widths and gaps—critical parameters for maximizing EA forces. As shown in Fig. 4a, Berdozzi et al. introduced inkjet printing of silver ink for EA device fabrication, citing advantages like high resolution, repeatability, and compatibility with various materials and geometries. This scalable, non-contact, and environmentally friendly process is suitable for both small-scale prototyping and large-scale industrial production<sup>17</sup>. As depicted in Fig. 4b, Kong et al. developed a silver nanowire (AgNW)-based ink for a 3D printing technique known as direct ink writing (DIW) and successfully printed AgNW electrode patterns on various substrates, including silicon, PET, and PI. The printed patterns demonstrated a very high resolution, with line widths as narrow as 50  $\mu\text{m}$ , and the final device achieved an adhesion stress of up to 15.5 kPa<sup>16</sup>. However, despite their processing advantages, conductive ink-based electrodes generally present common limitations including lower conductivity than bulk metals, environmental stability concerns, mechanical reliability issues during cyclic operation, and challenges in maintaining consistent electrical properties across different fabrication batches and operating conditions.

Liquid metal electrodes have emerged as a promising alternative that combines excellent conductivity with exceptional stretchability—a combination difficult to achieve with traditional solid conductors. Gallium-based liquid metals, such as eutectic gallium-indium (EGaIn) and gallium-indium-tin (Galinstan), maintain high conductivity even under significant deformation, making them particularly suitable for highly stretchable EA devices. These materials can be patterned through techniques like microfluidic embedding within elastomer channels. Park et al. demonstrated a stretchable EA device using interdigitated EGaIn microchannels embedded in PDMS, achieving excellent adhesion performance while preserving metallic conductivity during stretching<sup>66</sup>. Similarly, Kim et al. developed a soft capacitive sensor with EA capabilities using spider web-inspired liquid metal subsurface microwires, enabling both adhesion and sensing functions in a single device<sup>67</sup>. Despite their advantages, liquid metal electrodes face challenges including potential leakage, and more complex fabrication procedures compared to conventional electrode materials.

While thin metal layers on flexible substrates like PI provides adequate flexibility for certain applications, they generally prove unsuitable for stretchable devices. Metal electrodes, whether in film or particulate form, tend to develop cracks under strain, significantly compromising their conductivity. Additionally, metal electrodes face inherent challenges with oxidation over time. For these applications, carbon-based materials (CNTs, graphene, and carbon black) emerge as superior alternatives, either used independently or incorporated into polymer matrices. The simplest approach involves applying carbon particles directly onto elastomer surfaces using patterned masks, taking advantage of many elastomers' inherent surface adhesion properties. Among these materials, CNTs are particularly advantageous due to their ability to form conductive networks with minimal layer thickness and superior strain tolerance compared to alternative materials. Duduta et al. used a stamping method to apply CNTs onto a patterned mask, creating interdigitated electrode patterns<sup>68</sup>. The final EA device could be transferred to both curved and right-angled surfaces while maintaining pattern integrity, demonstrating good stability and flexibility. However, carbon-based electrodes also present significant limitations that must be considered for EA applications. These materials typically exhibit substantially lower conductivity compared to their metal counterparts. Carbon-based electrodes often face challenges with homogeneity and reproducibility during fabrication, leading to variability in device performance.

Carbon grease, consisting of carbon black dispersed in grease or silicone oil, represents another widely utilized carbon-based electrode material.



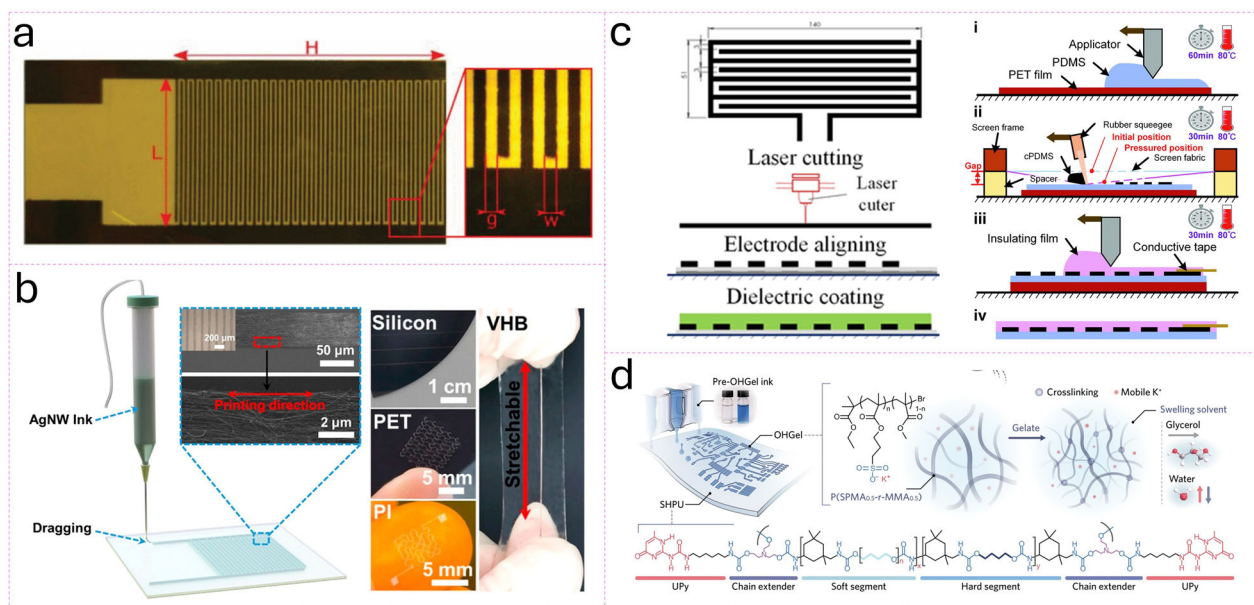


**Fig. 4 | Electrodes for soft EA device.** **a** Inkjet-printed metal electrode with high resolution. Reproduced with permission<sup>17</sup>. Copyright 2020 IEEE. **b** Direct ink writing-printed AgNWs electrode on various substrate. Reproduced with permission<sup>16</sup>. Copyright 2023 American Chemical Society. **c** Schematic diagram of the fabrication process of EA device with conductive silicone electrode. Reproduced

with permission<sup>59</sup>. Copyright 2019 Mary Ann Liebert, Inc. Reproduced under the Creative Commons Attribution 3.0 License (CC BY 3.0)<sup>15</sup>. Copyright 2018 IOP Publishing Ltd. **d** Inkjet-printed ionic conductor as the electrode of EA device. Reproduced under the Creative Commons Attribution 4.0 International License (CC BY 4.0)<sup>65</sup>. Copyright The Author(s) 2023.

Its non-solid nature minimizes mechanical constraints on stretchable substrates while maintaining conductivity under significant deformation, making it particularly suitable for applications combining DEA and EA functionalities. Wang et al. successfully implemented patterned carbon grease electrodes in an integrated DEA-EA gripper system, enabling both actuation and adhesion capabilities<sup>69</sup>. However, the practical challenges of handling carbon grease have led to increased interest in more manageable stretchable electrodes.

Stretchable conductive composites offer a more practical alternative, providing better stability and enhanced control over pattern geometry and thickness. These materials typically combine carbon black or CNTs with silicone-based precursors to create conductive elastomer matrices suitable for casting or printing into stretchable electrode patterns (Fig. 4c)<sup>15,59,70–74</sup>. The excellent mechanical properties of commercial silicones, combined with relatively low filler loading requirements, result in electrodes with exceptional stretchability, making them compatible with various soft actuators including pneumatic systems and DEAs. Furthermore, the availability of commercial conductive silicone sheets enables direct pattern creation through blade-cutting or laser-cutting processes<sup>75</sup>, making conductive elastomers currently the most prevalent and promising choice for stretchable EA applications. However, stretchable conductive composites face several inherent limitations. The incorporation of conductive fillers typically results in a significant trade-off between conductivity and mechanical properties, where higher filler concentrations improve electrical performance but compromise stretchability and mechanical durability. Additionally, they commonly suffer from strain-dependent resistance variations. Manufacturing challenges related to achieving uniform filler dispersion and consistent electrical properties across batches also remain significant barriers to their standardized implementation in commercial EA devices.

Recent developments in stretchable ionic conductors represent an emerging frontier in electrode materials for EA. Compared to traditional conductive elastomers incorporating carbon or metallic fillers, ionic conductive elastomers show potential for optical transparency, which might enable new possibilities in EA device applications. Moreover, these materials

provide enhanced tunability through matrix modification, as the matrix offers a wider range of choices and can be customized to achieve specific characteristics, such as a lower modulus, which could reduce constraints on soft actuators. Gao et al. developed a stretchable ionic conductor with innovative properties like self-healing, and the electrode can be inkjet-printed, allowing for the creation of smaller electrode widths and gaps, as shown in Fig. 4d<sup>65</sup>. However, ionic conductors are usually highly sensitive to environmental conditions such as humidity and temperature, which can dramatically alter their conductivity and operational stability. The long-term reliability of these materials remains a concern, as issues including electrolyte leakage, evaporation, or degradation may compromise performance over time.

Electrode patterning often relies on photolithography, laser scribing, or printing (e.g., screen or inkjet). Photolithography ensures high resolution but requires specialized facilities, multi-step chemical processing, and can be cost-intensive. Laser scribing is contactless and scalable, yet localized heat damage may occur on sensitive substrates. Printing methods generally provide a balanced trade-off among cost, speed, and resolution, though electrode conductivity can depend on ink formulation and post-treatment conditions. In all three approaches, complexity, throughput, and yield vary, so the final selection should consider device performance targets, substrate compatibility, and production volume. Typically, a compromise between high-resolution patterning and manufacturing scalability will determine the optimal fabrication route.

### Large-scale manufacturing

Achieving reliable large-scale manufacturing of EA devices requires thorough consideration of cost, reproducibility, and large-area patterning techniques. For instance, while additive manufacturing methods (e.g., inkjet printing and screen printing) can reduce material waste and enable flexible patterns<sup>17,65,76</sup>, maintaining uniform electrode gaps and dielectric thicknesses at industrial scales remain challenging due to the stringent precision needed to maximize EA performance. Subtractive and hybrid processes, such as chemical etching or laser ablation of large copper laminates, may provide repeatable electrode patterns over bigger areas, yet the associated

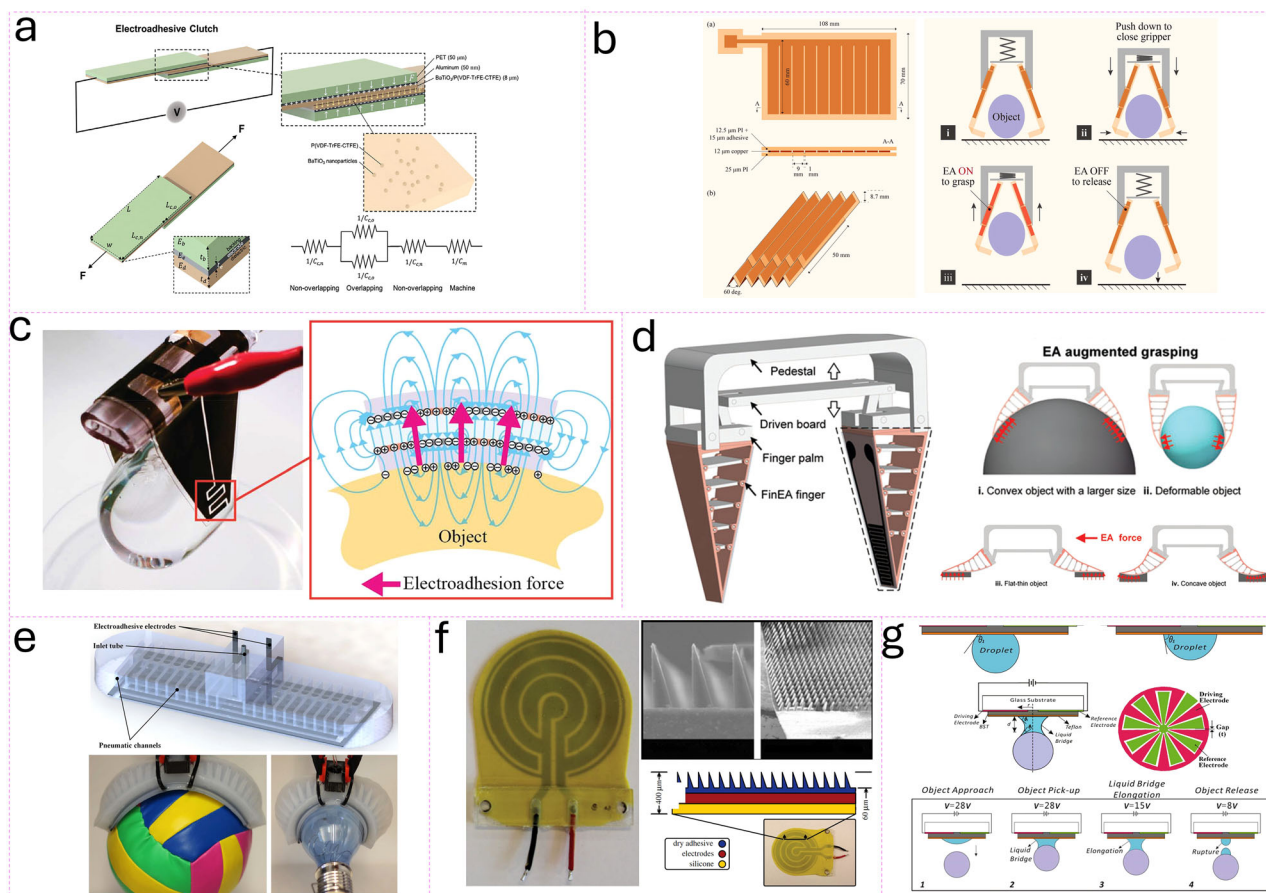


**Fig. 5 | EA technology is integrated into both clutches and grippers.** **a** The schematic illustrates a flexible clutch mechanism with an enhanced dielectric constant and its application for limiting joint rotation. Reproduced under the Creative Commons Attribution 4.0 International License (CC BY 4.0)<sup>139</sup>. Copyright 2024 The Authors. Advanced Materials Technologies published by Wiley-VCH GmbH. Reproduced with permission<sup>84</sup>. Copyright 2018 WILEY-VCH Verlag GmbH & Co. KGaA, Weinheim. **b** An origami-structured clutch-based gripper with high bending stiffness. Reproduced with permission<sup>140</sup>. Copyright 2023 IEEE. **c** A soft EA gripper integrated with a dielectric elastomer actuator (DEA) in a single structure. Reproduced with permission<sup>14</sup>. Copyright 2015 WILEY-VCH Verlag GmbH & Co. KGaA,

Weinheim. **d** EA patches combined with shape-adaptive soft robotic grippers to enhance grasping ability. Reproduced with permission<sup>59</sup>. Copyright 2019 Mary Ann Liebert, Inc. **e** The combination of pneumatic actuators with EA achieves a gripper with high grasping ability. Reproduced under the Creative Commons Attribution 3.0 License (CC BY 3.0)<sup>15</sup>. Copyright 2018 IOP Publishing Ltd. **f** A hybrid structure combining gecko-like adhesive with EA enhances the adhesive capabilities on both smooth and rough surfaces. Reproduced with permission<sup>37</sup>. Copyright 2014 Royal Society. **g** The microgripper, based on electrowetting, changes the contact angle of a water droplet to lift micro objects. Reproduced with permission<sup>90</sup>. Copyright 2009 IEEE.

tooling and setup costs can become significant when scaling up production<sup>5</sup>. Moreover, thin dielectric films that offer higher EA forces must be processed in carefully controlled environments to prevent surface defects and ensure consistent breakdown strengths across large area. Balancing manufacturing throughput with uniform quality is essential for scaling up EA technologies. Future efforts may benefit from adopting advanced fabrication strategies such as roll-to-roll printing, which have shown potential in related flexible electronics domains<sup>77</sup>. By improving patterning consistency and material integration efficiency, these approaches could reduce fabrication defects and enable more scalable and economically viable EA device production for industrial applications.

## Applications of electroadhesion in soft robotics

### Clutch

EA brakes represent an innovative braking technology that utilizes EA to generate strong adhesion forces during the braking process<sup>78–80</sup>. The primary mechanism involves applying an electric field between two surfaces, which creates a significant attractive force when voltage is applied, as shown in Fig. 5a. This force effectively binds the brake components together, leading to significant braking capability. A key advantage of EA-based brakes is their quick response time (10 to 100 milliseconds)<sup>81</sup>. The rapid adjustment of adhesion strength enables more precise and immediate braking. Moreover,

the substantial adhesion generated provides enhanced stopping power, surpassing traditional mechanical brakes. Additionally, EA brakes feature low energy consumption. Unlike conventional braking systems that rely on mechanical friction, EA brakes operate efficiently, minimizing energy requirements during braking. This makes them ideal for electric vehicles and automated systems. EA-based brakes are applied in fields such as electric vehicles<sup>82</sup>, industrial robots<sup>5</sup>, and automation equipment<sup>83</sup>, where efficient and reliable braking is crucial.

Advancements in technology and user demands have shifted EA clutches from rigid to more flexible and soft designs. This evolution has facilitated their integration into applications such as wearable devices and soft robotics, thereby enhancing their versatility and adaptability in various fields. As depicted in Fig. 5a, electrodes are deposited onto textile substrates, and the dielectric materials are constructed from flexible organic compounds<sup>84</sup>. This design enables the creation of a flexible EA clutch, enhancing its suitability for wearable devices. Another research focus for EA clutches is reducing the active voltage required for shear force generation. Even with the use of composite materials in the design of the dielectric layer, the active voltage still ranges from several hundred to several kilovolts. The incorporation of polyelectrolytes can reduce the active voltage to 5 V<sup>85</sup>, leveraging the benefits of the ionic double layer (IDL) effect. One disadvantage of polyelectrolyte-based low-voltage EA clutches is the prolonged

release time due to residual charges. Most EA clutches only bear shear forces parallel to the tensile load, rendering them weak against compressive forces and moments. Recently, a 3D structured EA clutch inspired by origami has achieved a significant improvement in stability under compression, as illustrated in Fig. 5b. Because EA clutches lack actuation capability, they are combined with other actuators like pneumatic actuators, dielectric elastomer actuators, and ionic polymer metal composites in soft robotics. Integrating EA clutches with different actuators holds promise for advancements in soft robotics.

### Gripper

Another prominent application of EA is its use as a gripper, adaptable across a spectrum from rigid to flexible and soft materials<sup>86–88</sup>. The gripper utilizes the large shear force generated by EA, allowing it to easily achieve a grasping capability of several tens of kilograms. Since the normal force between the EA patch and the target objects is confined to the surfaces of the objects, this type of gripper minimizes the risk of damage to them. While the EA gripper exhibits a significant blocking force, its available actuation mechanisms offer limited precision in positioning the target point. The first method to address the aforementioned problem is to combine dielectric elastomer actuators (DEAs) with EA. In the work of Shintake et al. two pairs of finger electrodes are arranged and wrapped with dielectric materials<sup>14</sup>, as shown in Fig. 5c. The two layers of active finger electrodes squeeze the middle layer of dielectric polymer to elongate it. The dielectric layer near the pair of finger electrodes, used for EA, is somewhat thick, causing the extension strain to be transferred to bending. EA is also combined with a shape-adaptive gripper to enhance its capability for grasping large objects as well as thin, lightweight items<sup>59</sup>. Chen et al. positioned the EA patch on the interior of the adaptive gripper finger, as illustrated in Fig. 5d. The adaptive gripper is effective at grasping objects of various shapes when the objects are suitable for the gripper fingers' wrapping. When the object is large, the gripper may squeeze the object out due to insufficient shear force; EA patch serves as a valuable supplement in this situation. This strategy is also applied by combining the pneumatic gripper with EA, yielding results similar to those obtained with the combination of the adaptive gripper and EA in the work of Guo et al.<sup>15</sup>, as shown in Fig. 5e.

An intriguing technology reported in the literature utilizes EA to enhance the adhesion properties of gecko-inspired adhesives on rough surfaces<sup>37</sup>, as shown in Fig. 5f. The electrostatic force generated by the EA layer exerts increased pressure on this gecko-inspired adhesive, enhancing its contact with the target object and increasing the contact area to generate greater van der Waals adhesion force. In an EA clutch, EA function can facilitate the development of a gripper with tunable stiffness<sup>89</sup>. In the work of Chen et al., multiple pairs of flexible EA clutches are systematically arranged in layers to constitute the gripper finger. By selectively activating different numbers of clutches, it is possible to achieve a range of stiffness levels. Low stiffness enhances the effective contact between EA and the objects, whereas high stiffness serves to maintain this contact, thereby enabling the attainment of a stable blocking force. Electrowetting, a form of EA, involves applying an electric charge to a droplet to modify the adhesive force between it and the substrate. This process controls the contact angle, enabling better manipulation of liquid on surfaces. Vasudev et al. have reported micro-gripper that utilizes water droplets for adhesion and release of objects<sup>90</sup>, as illustrated in Fig. 5g. Initially, the droplet has a large contact angle, allowing contact with the object for lifting. Upon activation, electrowetting reduces the contact angle, allowing the object to be released.

### Robotics

EA technology has emerged as a key innovation in robotics, enabling robots to adhere to various surfaces with adjustable force. This capability enhances the versatility of robotic systems in applications such as climbing and resting on different object surfaces. The primary application of EA in robotics involves emulating the adhesion mechanisms of birds or reptiles, enabling the robots to maintain a stable position at a single point for resting. For this application, a single EA patch is typically sufficient to generate the necessary

adhesion force for fixation and to deactivate for release. The EA patch is positioned on the head of the robotic insect<sup>22</sup>, as shown in Fig. 6a. Upon approaching the target location, the patch is activated to generate the necessary adhesion force for secure attachment to the surface<sup>22</sup>. The robotic system designed to achieve crawling functionality with feet encounters the challenge of generating variable friction forces at the feet to facilitate locomotion. EA presents a viable solution to this challenge, owing to its capability to provide adjustable adhesion forces. As illustrated in Fig. 6b, in the work of Gu et al. the clawing robot is equipped with a dielectric elastomer actuator (DEA) to produce bending strain, which serves as the basis for clawing deformation<sup>53</sup>. Additionally, it incorporates two EA patches as feet to generate alternating friction forces. The hind feet are activated to generate frictional force, after which the DEA is engaged to extend the forefoot by a specified length. Subsequently, the forefoot is activated to secure its position, while the hindfoot is deactivated to release the adhesion. At this juncture, the DEA is deactivated, resulting in the bending of the insect's back and the forward extension of the hindfoot. The configuration of two feet facilitates clawing functionality in a single direction, thereby limiting the capability to change direction. Augmenting the number of EA feet will enhance the agility of the robots and improve their capacity for directional change<sup>91</sup>, as shown in Fig. 6c. This robot is equipped with four EA feet, featuring an adjustable activation sequence to modify the locomotion model. The foot of the robotic system can be designed in a crawler configuration and activated in a specified sequence. A crawler foot and a brushless motor are integrated into a unified structure to facilitate locomotion<sup>21</sup>, as shown in Fig. 6d. The belt crawler foot rotates to enable forward and backward locomotion, while the electrostatic force generated between the crawler and the body electrode film supplies the requisite force for movement.

### Haptic device

Haptic technology focuses on the sense of touch and provides tactile feedback to users, enhancing their interaction with digital environments. Its applications range from virtual reality and gaming to medical training and remote robotics, allowing for a more immersive and intuitive user experience. In contrast to EA clutches and feet in robotics that utilize direct current (DC) to generate adhesion forces, EA employed in haptic devices predominantly relies on alternating current (AC)<sup>24,92</sup>. The main structure of the tactile screen consists of an electrode covered by a dielectric layer<sup>46,93</sup>, as shown in Fig. 6e. EA in tactile screens operates by using electric fields to create adhesion between the screen's surface and the user's finger, enhancing the tactile feedback experienced during interaction. Key control factors include the magnitude of the applied voltage, the surface material properties, and the dielectric layer's thickness, all of which influence the strength and responsiveness of the EA interaction. One significant challenge of EA in tactile screens is the limited effectiveness of adhesion at higher speeds or rapid interactions, which can lead to a less responsive user experience. Additionally, the need for precise control of voltage levels to prevent overheating or damaging the dielectric layer can complicate the design and implementation of these systems.

A 2.5 D haptic device has been reported that does not directly employ EA between the electrode and the human finger. The haptic device employs an array of metal rods arranged in various configurations to create distinct patterns and text, enabling users to sense these elements with their fingers to obtain information<sup>94</sup>, as shown in Fig. 6f. The rods are elevated by the underlying platform, and as the platform descends, the rods are secured at the designated height by EA clutches, facilitating the formation of patterns and text. This 2.5 D tactile device encounters challenges related to efficiency and is constrained in its capacity to process large data sets.

### Electrostatic cleaning and sealing

AC electrostatic cleaning utilizes an alternating current to generate an electric field that effectively removes contaminants from surfaces. In this method, the alternating current induces periodic changes in the electric field, causing the contaminants to experience varying polarities, which generates attractive or repulsive forces<sup>95,96</sup>. This interaction



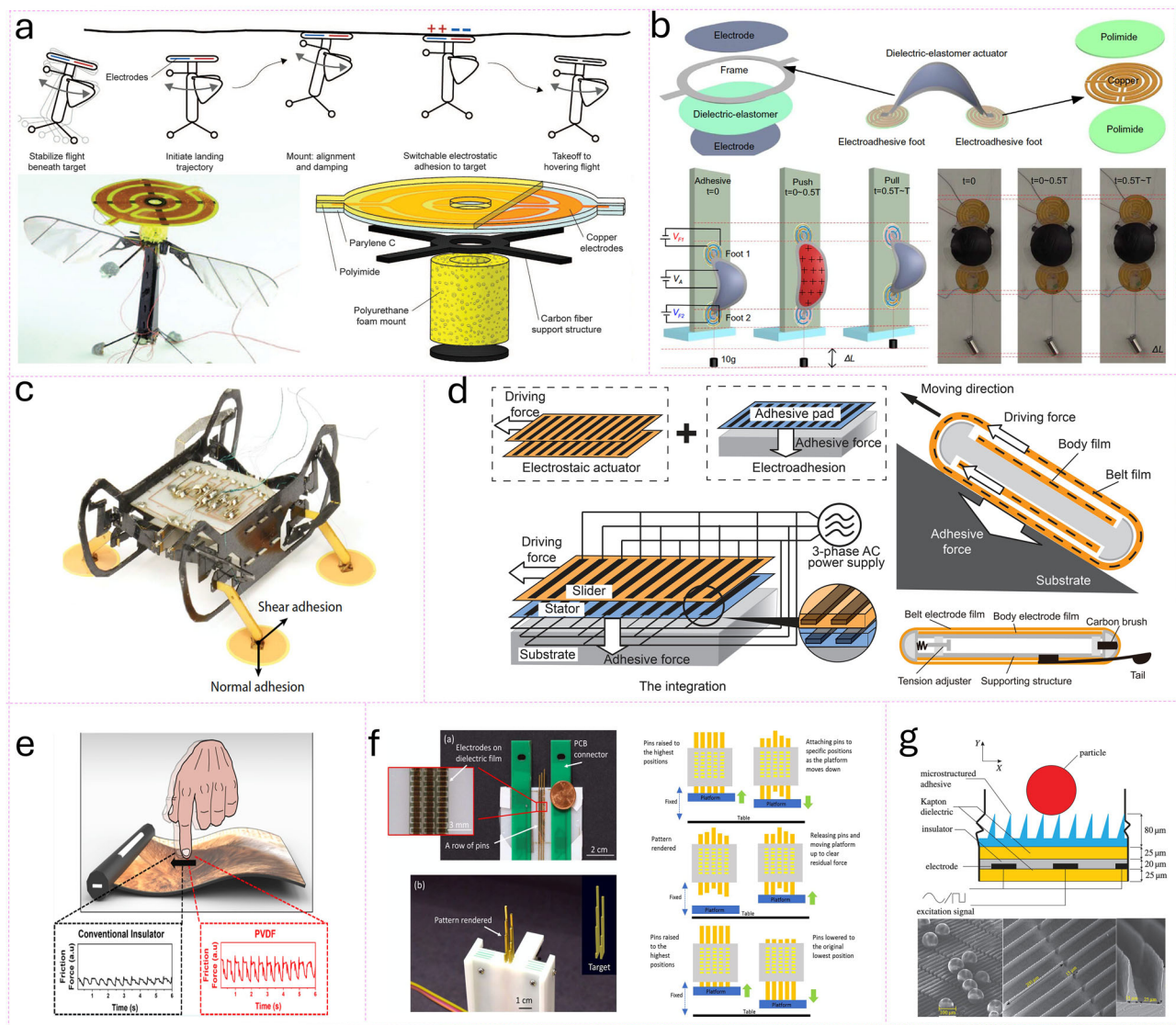


**Fig. 6 | EA technology is integrated into robotics, haptic sensors, and self-cleaning applications.** **a** Landing and launching of a robotic insect on overhangs using adjustable EA. Reproduced with permission<sup>22</sup>. Copyright 2016, American Association for the Advancement of Science. **b** EA patches employed as adhesion mechanisms for soft wall-climbing robots. Reproduced with permission<sup>53</sup>. Copyright 2018, The American Association for the Advancement of Science. **c** Utilizing EA technology for inverted and vertical locomotion of quadrupedal microrobots. Reproduced with permission<sup>91</sup>. Copyright 2018, The American Association for the Advancement of Science. **d** A climbing crawler robot that integrates EA for its foot

mechanism and employs a flexible electrostatic motor. Reproduced under the Creative Commons Attribution 3.0 License (CC BY 3.0)<sup>21</sup>. Copyright 2014 The Author(s). **e** Contact mechanics between the human finger and a touchscreen facilitated by EA and enhanced through the incorporation of PVDF. Reproduced with permission<sup>93</sup>. Copyright 2024, American Chemical Society. **f** Electrostatic adhesive braking mechanisms for advanced high spatial resolution refreshable 2.5D tactile shape display systems. Reproduced with permission<sup>94</sup>. Copyright 2018, IEEE. **g** AC voltage-triggered EA utilized for the cleaning of gecko-inspired adhesives. Reproduced with permission<sup>97</sup>. Copyright 2018, Royal Society.

allows for the effective removal of dust, grease, and other small particles from the surface, making it particularly suitable for cleaning delicate and intricate components. The technique offers advantages such as high cleaning efficiency and the absence of chemical agents. In the work of Alizadehyazdi et al. a gecko-inspired dry adhesion technique has been reported in conjunction with electrostatic cleaning technology<sup>97</sup>. The gecko-inspired structure exhibits a high sensitivity to dust, which markedly reduces the adhesion force. With the application of an AC high-voltage signal, the dust will become polarized and be removed from the surface. AC electrostatic cleaning has several drawbacks that should be considered. Its effectiveness can be sensitive to environmental conditions, such as humidity and temperature, as moisture may interfere with electrostatic forces. Additionally, while it works well for dust and small particles, it may not efficiently remove heavier or oily residues that require mechanical cleaning. Safety concerns arise from the use of

high-voltage AC signals, necessitating careful handling to prevent electrical hazards. Furthermore, the technology can involve complex equipment and maintenance, increasing operational costs, and not all surfaces may be compatible, particularly those that are highly conductive or have coatings susceptible to electrical stress.

EA has been identified as a valuable technique for sealing suction cups, which necessitate preliminary sealing to enable subsequent vacuum adhesion. In the work of Okuno et al. the EA ring is integrated into the edge of the suction cup. Upon contact with an object, the EA ring exerts pressure, facilitating a seal that enhances the effectiveness of the suction mechanism<sup>71</sup>. EA enhances the performance of suction cups by providing a reliable seal that improves adhesion to various surfaces, including porous or uneven materials. Additionally, it allows for greater control over the adhesion force, enabling the suction cup to be easily activated or deactivated as needed, which increases its versatility in applications.

## Space application

EA technology has emerged as a compelling solution for on-orbit tasks, offering the potential to tackle longstanding challenges in space operations that stem from vacuum conditions, extreme temperature fluctuations, and radiation exposure. By leveraging electrostatic forces rather than conventional mechanical clamping methods, EA devices exhibit low energy consumption, minimal structural complexity, and no chemical byproducts, thus enabling gentle yet robust adhesion on diverse spacecraft materials<sup>34</sup>. Early tests at NASA's Marshall Space Flight Center illustrated that carefully engineered EA pads can function reliably in reduced-pressure test chambers, providing strong clamping forces with minimal current draw even on curved or uneven satellite components<sup>4</sup>. These fundamental demonstrations were further substantiated by flight experiments under microgravity conditions, which showed that the absence of a stable gravitational field does not undermine EA's capacity to form and maintain contact<sup>98</sup>.

Researchers have deployed electroadhesive (EA) mechanisms across the aerospace sector in distinct operational categories. Material manipulation represents the first key domain, with several works validating item acquisition devices for transfer tasks simulated spacecraft environment<sup>99,100</sup>. Expanding this functionality, Saravia et al. engineer an adaptable capture unit merging fiber-composite structures with polarizable surfaces tailored for collecting space refuse<sup>101</sup>. Extending these innovations, Leung et al. validated EA grippers for spacecraft docking and servicing within vacuum chambers and frictionless-plane simulations<sup>102</sup>. Similarly, Ritter et al. characterized geometry-based variations of EA devices, demonstrating how different shapes and electrode designs can optimize shear adhesion on substrates like aluminum and aluminized films, thereby broadening the potential for agile capture mechanisms in space-based missions<sup>103</sup>.

## Challenges and future directions

### Reducing high voltage requirement

The intense electric field present in electroadhesion (EA) devices poses significant challenges despite the typically low leakage current—often limited to a few microamperes—which helps maintain low power consumption. These high fields can cause dielectric breakdown, field emission, and long-term material degradation, particularly near sharp features or thin insulating regions. Additionally, excessive electric fields can induce electrochemical reactions or mechanical instabilities, especially in soft robotic applications involving stretchable or compliant materials. These effects not only threaten device reliability and user safety but also limit EA's integration into real-world, safety-critical systems. Therefore, managing the electric field—by optimizing electrode geometry, improving dielectric strength, or enhancing material properties—has become a central research objective aimed at extending the functionality and safety of EA devices across broader application domains.

Improvements in device design can help by adjusting factors like electrode spacing or reducing dielectric thickness<sup>4</sup>. However, reducing electrode gaps is limited by the breakdown of the dielectric material and current electrode fabrication precision, and thinner dielectric films may lead to durability issues, potentially impacting performance and longevity<sup>104</sup>. Optimizing dielectric materials by increasing their dielectric constant represents another promising approach, as materials with higher constants can achieve greater adhesion force at lower voltages. For example, PVDF-based materials with high dielectric constants (exceeding 50) have been shown to reduce operational voltages, with research of Ranjithkumar et al. demonstrating an EA device that operated at just 250 V using high-dielectric PVDF-based material<sup>57</sup>.

In stretchable EA applications, researchers predominantly utilize commercially available materials, primarily silicone elastomers<sup>14,15,105</sup>. Despite their excellent mechanical properties, silicones like PDMS and Ecoflex exhibit relatively low dielectric constants (typically below 3). While there is ongoing research into high-dielectric-constant elastomers, few have been adapted specifically for EA applications, with most being tailored for dielectric elastomer actuators<sup>60,106,107</sup>. Several new polymers have been formulated to create elastomers with enhanced dielectric properties, such as

high dielectric constants, strong dielectric strength, and desirable mechanical characteristics<sup>106,108</sup>. Another simpler method to increase dielectric constants is introducing fillers—such as metal, ceramic, ionic conductors, or carbon, etc.—into the polymer matrix, as shown in Fig. 7a<sup>61,109–112</sup>. These novel materials and approaches could probably reduce the operational voltage requirements for EA devices. However, careful consideration must be given to the trade-off between enhanced dielectric constant and potential degradation of mechanical and dielectric strength at higher filler concentrations<sup>109</sup>.

### Achieve fast adhesion and de-adhesion

EA exhibits a complex and dynamic electrostatic attraction effect characterized by time-dependent behavior<sup>5</sup>. When the system is activated, residual charges trapped within the EA dielectric require a finite period to reach maximum adhesive force, and similarly, a finite duration is needed for force dissipation when the system is deactivated. In most applications, a faster adhering and releasing process is preferable, necessitating the development of methods to accelerate both the adhesion and de-adhesion processes. To enhance adhesion speed, one effective solution is to temporarily apply a higher voltage than is required to generate the desired force, then lower the voltage to a maintenance level sufficient to sustain that force.

Various methods for rapid de-adhesion have been proposed, typically falling into mechanical and electrical approaches. Mechanical solutions incorporate additional components, predominantly soft actuators, into the EA device to create movement that assists with releasing the adhered object, often making the EA systems more complex but enabling nearly instantaneous release. For instance, in grippers that integrate soft actuators with EA devices, the actuator movement can assist in peeling the EA device from the surface even when the adhesion force has not fully dissipated. Many works incorporate soft actuators specifically for fast releasing, often using them in a vibration mode. As depicted in Fig. 7b, Gao et al. for example, utilized resonant vibrations from embedded dielectric elastomer actuators for quick release<sup>72</sup>, and similarly, Xiang et al. developed a pneumatic-driven vibration method to expedite EA release<sup>62</sup>. In terms of electrical approaches, advanced voltage control methods and associated electronics have been employed, including oscillatory release waveforms (10–100 Hz), adaptive release voltages, exponentially decaying reverse-polarity voltages (50–80% of adhesion voltage), and variable polarity voltage techniques. These methods have significantly advanced the rapid de-adhesion capabilities of EA systems<sup>5</sup>. Nonetheless, there remains a need for a cost-effective, easy-to-implement, lightweight, and durable solution for quick EA de-adhesion that is compatible with all types of materials.

### Incorporate sensing capabilities

Integrating sensing functions into EA devices is highly advantageous. Since EA devices fundamentally operate as capacitors, often with interdigital electrode patterns, their structure is closely aligned with that of capacitive sensors<sup>67</sup>. Although EA devices operate effectively across a broad range of surfaces, encompassing diverse materials and textures, the adhesion force they generate is subject to significant variation due to numerous factors, including the material properties of the object, its surface conditions, and environmental influences such as temperature and humidity<sup>4,5</sup>. Consequently, integrating sensing functions into EA systems becomes crucial, enabling them to adapt more dynamically and perform with greater precision.

Guo et al. developed an EA-DEA gripper with proprioceptive and exteroceptive capabilities. As shown in Fig. 7c. The proprioceptive feature allows the gripper to sense its own deformations, while exteroceptive sensing enables the gripper to differentiate between the types of surfaces it contacts. These integrated sensing capabilities significantly improve the gripper's functionality and adaptability in robotic applications<sup>113</sup>. In their another work on EA-pneumatic gripper, he also designed a stretchable touch sensor and integrate it on the gripper to sense whether the object is gripped, making the gripper more controllable and intelligent<sup>15</sup>. Similarly, Gao et al. also used his EA device as a capacitive sensor to sense the location of the object and

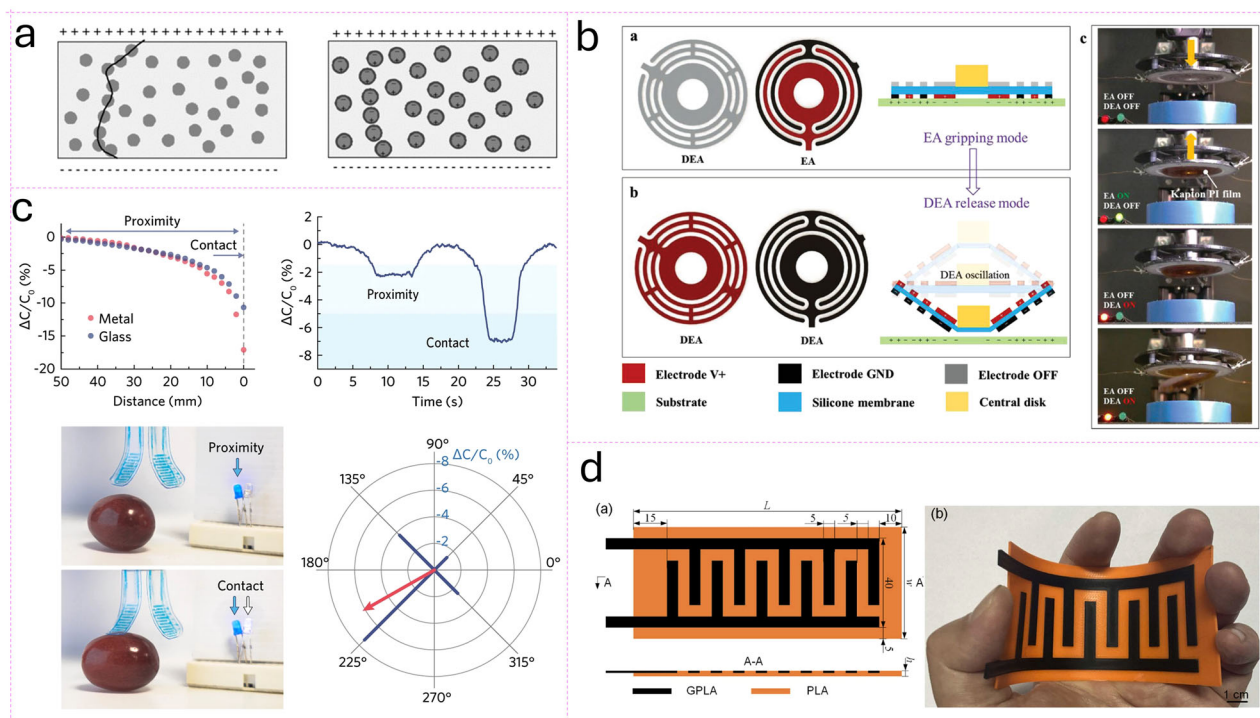


**Fig. 7 | Some future directions for EA device.** **a** Increasing dielectric constant of the dielectric materials by introducing fillers. Reproduced with permission<sup>111</sup>. Copyright 2010 WILEY-VCH Verlag GmbH & Co. KGaA, Weinheim. **b** Fast release of the EA device with the assistance of vibration of DEA. Reproduced with permission<sup>72</sup>. Copyright 2018 WILEY-VCH Verlag GmbH & Co. KGaA, Weinheim. **c** EA gripper

integrated with the capability of sensing the location of the object. Reproduced under the Creative Commons Attribution 4.0 International License (CC BY 4.0)<sup>65</sup>. Copyright The Author(s) 2023. **d** Fully 3D-printed EA device. Reproduced with permission<sup>114</sup>. Copyright 2022 Elsevier B.V.

distinguish if the object is in proximity or in contact, demonstrating the multi-functional potential of EA devices<sup>65</sup>.

### Advanced fabrication methods

In the fabrication of EA devices, minimizing electrode gaps can enhance EA performance, making high-resolution fabrication methods essential. Many advanced fabrication methods including laser cutting and inkjet printing have been introduced into the fabrication of EA devices, offering scalable precision up to micro scales, critical for tuning EA performance<sup>17,65</sup>. These advanced fabrication methods continue to improve EA device performance by enabling finer control over structural details.

Inkjet printing, for example, offers exceptional flexibility in creating complex electrode patterns with line widths down to 50  $\mu\text{m}$ <sup>17,65</sup>. This technique provides not only high resolution but also scalability from laboratory prototyping to industrial production, while maintaining environmental advantages through reduced material waste. These advanced fabrication methods enable micrometer-scale precision in electrode patterning, resulting in EA devices with optimized electric field distributions and higher adhesion forces.

Optical fabrication methods (including photolithography, laser-based patterning, and related high-resolution processes) represent another highly promising route for producing dense, interdigitated electrodes with feature sizes below the capabilities of many additive manufacturing systems. By leveraging precisely controlled exposure and etching steps, optical methods can achieve sub-micrometer pattern fidelity and faster throughput in certain batch-fabrication settings, making them an attractive option when both feature precision and large-volume production are required. These techniques are particularly valuable for applications requiring extremely precise electrode geometries to maximize adhesion force while minimizing operational voltage.

Another key challenge in EA device fabrication involves the current practice of using distinct methods for creating the dielectric and electrode materials, often requiring manual handling and complicating the process. For EA devices integrated with actuators, separate fabrication of each component is typical, followed by manual assembly. Currently, few approaches successfully integrate both components into a single, dual-function device. However, 3D printing offers a promising solution, as it can not only control dielectric thickness but also print precise electrode patterns as shown in Fig. 7d<sup>114</sup>. This approach enables single-step device fabrication, particularly as multi-material 3D printing has demonstrated the capability to create both dielectric and conductive layers simultaneously<sup>76,115,116</sup>. Furthermore, because 3D printing is already widely employed in fabricating various kinds of soft actuators<sup>117–123</sup>, incorporating it into EA device fabrication could support seamless integration of EA devices with soft actuators, potentially revolutionizing the manufacturing process for complex EA systems.

The convergence of these advanced fabrication technologies—from high-resolution printing and optical methods to multi-material 3D printing—provides a robust foundation for addressing current limitations in EA device performance and integration, ultimately expanding their potential applications in soft robotics and beyond.

### Ionic-based electroadhesion

Recently, a novel approach to EA based on ionic materials has shown great promise by enabling strong adhesion at remarkably low voltages. Unlike traditional dielectric EA which requires kilovolt-range potentials, ionic EA can operate effectively at voltages as low as 1–10 V<sup>124,125</sup>. The key mechanism relies on heterojunctions between ionoelastomers of opposite polarity, where a molecular-scale ionic double layer (IDL) forms at the interface<sup>124</sup>. When operated under reverse bias, mobile ions are pulled away from the interfacial region, leading to a build-up of excess fixed charges in the IDL.



The electric field generated by these excess fixed charges in the thin interfacial layer induces electrostatic adhesion. Under forward bias, mobile cations are driven from the polyanion domain into the polycation domain (and vice versa for mobile anions), causing the interface to behave resistively and thus losing the electrostatic adhesion<sup>85,124</sup>. State-of-the-art ionic EA systems can achieve adhesion forces up to 102 N/cm<sup>2</sup> at 7.5 V, with less than 7% variation in charge storage capability after 1000 cycles<sup>85</sup>. Compared to conventional dielectric-based adhesion, ionic systems offer several advantages including significantly lower operating voltages, higher force capacity per unit stored energy, and remarkable tolerance to defects or damage<sup>124</sup>. However, the ionoelastomer material system usually has longer charging time than the other EA system, due to the viscoelastic effects that occur during charging.

### Hybrid electroadhesion systems

Recent advances in robotics have witnessed increasing interest in hybrid approaches that combine EA with complementary adhesion technologies to overcome individual limitations and enhance overall performance. The synergy between EA and other mechanisms, such as gecko-inspired adhesives and DEAs, has shown remarkable performance improvements. Integrating EA with DEAs creates multifunctional systems capable of both shape adaptation and controllable adhesion, as shown in Shintake's work on soft grippers that can delicately handle fragile objects<sup>14</sup>.

Gecko-inspired dry adhesives combined with EA demonstrate enhanced shear adhesion strength on both smooth and rough surfaces, leveraging the van der Waals forces of micro/nanoscale features and the electrostatic attraction of EA. As demonstrated by Ruffatto et al., this hybrid approach achieves up to five times greater shear adhesion compared to either technology alone, with improved performance across diverse surface materials<sup>37</sup>.

Hybrid configurations that incorporate pneumatic actuators with EA pads offer comparable benefits. Because pneumatic actuators can deform significantly under pressure, they ensure a large and conformal contact area between the electroadhesive pad and the target object, which is crucial for establishing strong adhesion forces. One example is the combination of a soft pneumatic finger and an electroadhesive patch: once the pneumatic actuator inflates and wraps around an item, the electroadhesive pad is activated to provide additional shear force and reduce slippage, as illustrated by Guo et al. in a shape-adaptive gripper design<sup>15</sup>. This approach leverages the strong normal pressure generated by the pneumatic inflation to maximize intimate contact, and then supplements the grip with controllable electrostatic adhesion for improved precision and load-carrying capacity. As a result, the hybrid system can lift heavier or more slippery objects than either pneumatic gripping or EA alone, while maintaining relatively low power usage and gentle handling.

In liquid manipulation, electrowetting-based techniques serve as another promising complement to EA. Electrowetting, often regarded as a form of EA for liquids, modifies the contact angle of a droplet through an applied voltage and thus enables more efficient droplet displacement and handling. By inserting interdigitated electrodes beneath a hydrophobic dielectric layer, researchers can cause droplets to migrate or deform, allowing them to function as microfluidic "grippers." In one such example, Vasudev and Zhe developed a microgripper in which a water droplet's contact angle is reduced via electrowetting, thereby controlling capillary forces to lift and release micro-scale objects<sup>90</sup>. Combining EA for solid interfaces with electrowetting for liquid interfaces suggests a future where multi-phase manipulation (both solids and fluids) can be integrated in a single soft robotic platform. This opens up new possibilities for applications requiring rapid switching between solid object manipulation and fluidic transport, such as biomedical or lab-on-a-chip systems.

These hybrid approaches represent a significant advancement in addressing the inherent limitations of standalone EA systems, particularly in applications requiring robust adhesion across various environmental conditions, improved force-to-weight ratios, or faster adhesion/de-adhesion cycles. The continued development of such hybrid systems will likely

expand the application scope of EA technology in fields ranging from space robotics to medical devices.

### Conclusion

This review has comprehensively examined the development and application of EA technology in soft robotics, highlighting its significant potential as a controllable and versatile adhesion mechanism. The fundamental principles of EA, including both Maxwell stress and Johnsen-Rahbek effects, have been thoroughly investigated, providing a theoretical foundation for device optimization. Through systematic analysis of influential variables such as electrode field, surface roughness, electrode patterns, and environmental factors, researchers have gained deeper insights into optimizing EA performance for specific applications.

Significant progress has been made in materials development and fabrication techniques for EA devices. The emergence of flexible and stretchable dielectric materials has enabled the seamless integration of EA with soft robotic systems. Advanced electrode materials and fabrication methods, ranging from metallic electrode to carbon-based composites and innovative ionic conductors, have further enhanced capabilities of EA devices. These developments have facilitated diverse applications in soft robotics, including clutches, grippers, climbing robots, and haptic interfaces, demonstrating the versatility of EA technology.

Despite these advances, several challenges remain to be addressed for wider adoption of EA technology. These include reducing operational voltage requirements, achieving faster adhesion/de-adhesion responses, incorporating sensing capabilities, and developing more efficient fabrication methods. Looking forward, the continued development of multifunctional materials, integration of sensing capabilities, and advancement in fabrication technologies will likely drive the next generation of EA devices, potentially revolutionizing soft robotics applications.

### Data availability

No datasets were generated or analysed during the current study.

Received: 10 January 2025; Accepted: 26 July 2025;

Published online: 03 September 2025

### References

1. Rus, D. & Tolley, M. T. Design, fabrication and control of soft robots. *Nature* **521**, 467–475 (2015).
2. Shintake, J., Cacucciolo, V., Floreano, D. & Shea, H. Soft Robotic Grippers. *Adv. Mater.* **30**, 1707035 (2018).
3. Zhou, J., Chen, S. & Wang, Z. A Soft-Robotic Gripper With Enhanced Object Adaptation and Grasping Reliability. *IEEE Robot. Autom. Lett.* **2**, 2287–2293 (2017).
4. Rajagopalan, P. et al. Advancement of Electroadhesion Technology for Intelligent and Self-Reliant Robotic Applications. *Adv. Intell. Syst.* **4**, 2200064 (2022).
5. Guo, J., Leng, J. & Rossiter, J. Electroadhesion Technologies for Robotics: A Comprehensive Review. *IEEE Trans. Robot.* **36**, 313–327 (2020).
6. Guo, J., Bamber, T., Chamberlain, M., Justham, L. & Jackson, M. Optimization and experimental verification of coplanar interdigital electroadhesives. *J. Phys. Appl. Phys.* **49**, 415304 (2016).
7. Ruffatto, D., Shah, J. & Spenko, M. Increasing the adhesion force of electrostatic adhesives using optimized electrode geometry and a novel manufacturing process. *J. Electrostat.* **72**, 147–155 (2014).
8. Monkman, G. J. An analysis of astrictive prehension. *Int. J. Robot. Res.* **16**, 1–10 (1997).
9. Guo, J. et al. Toward Adaptive and Intelligent Electroadhesives for Robotic Material Handling. *IEEE Robot. Autom. Lett.* **2**, 538–545 (2017).
10. Nakamura, T. & Yamamoto, A. Modeling and control of electroadhesion force in DC voltage. *ROBOMECH J* **4**, 1–10 (2017).
11. Diller, S., Majidi, C. & Collins, S. H. A lightweight, low-power electroadhesive clutch and spring for exoskeleton actuation. In 2016

- IEEE International Conference on Robotics and Automation (ICRA)* 682–689 (IEEE, Stockholm, Sweden, 2016). <https://doi.org/10.1109/ICRA.2016.7487194>.
12. Krinsky, E. & Collins, S. H. Elastic energy-recycling actuators for efficient robots. *Sci. Robot.* **9**, eadj7246 (2024).
13. Caruso, F., Shea, H. & Cacciucolo, V. Electroadhesion Suction Cups. *Adv. Mater.* **n/a**, 2420231.
14. Shintake, J., Rosset, S., Schubert, B., Floreano, D. & Shea, H. Versatile Soft Grippers with Intrinsic Electroadhesion Based on Multifunctional Polymer Actuators. *Adv. Mater.* **28**, 231–238 (2016).
15. Guo, J. et al. Soft pneumatic grippers embedded with stretchable electroadhesion. *Smart Mater. Struct.* **27**, 055006 (2018).
16. Kong, X. et al. Direct Writing of Silver Nanowire Patterns with Line Width down to 50  $\mu\text{m}$  and Ultrahigh Conductivity. *ACS Appl. Mater. Interfaces* **15**, 9906–9915 (2023).
17. Berdozzi, N. et al. Rapid Fabrication of Electro-Adhesive Devices With Inkjet Printed Electrodes. *IEEE Robot. Autom. Lett.* **5**, 2770–2776 (2020).
18. Guo, J. et al. Experimental study of a flexible and environmentally stable electroadhesive device. *Appl. Phys. Lett.* **111**, 251603 (2017).
19. Hwang, G., Park, J., Cortes, D. S. D. & Kyung, K.-U. Mechanically Strengthened Electroadhesion based Soft Gripper with Multi-layered Dielectric Elastomer Actuator. In *2020 3rd IEEE International Conference on Soft Robotics (RoboSoft)* 748–753 (2020). <https://doi.org/10.1109/RoboSoft48309.2020.9116048>.
20. Wei, D. et al. Electrostatic Adhesion Clutch with Superhigh Force Density Achieved by MXene-Poly(Vinylidene Fluoride–Trifluoroethylene–Chlorotrifluoroethylene) Composites. *Soft Robot* **10**, 482–492 (2023).
21. Wang, H., Yamamoto, A. & Higuchi, T. A Crawler Climbing Robot Integrating Electroadhesion and Electrostatic Actuation. *Int. J. Adv. Robot. Syst.* **11**, 191 (2014).
22. Graule, M. A. et al. Perching and takeoff of a robotic insect on overhangs using switchable electrostatic adhesion. *Science* **352**, 978–982 (2016).
23. Basdogan, C., Sormoli, M. R. A. & Sirin, O. Modeling Sliding Friction Between Human Finger and Touchscreen Under Electroadhesion. *IEEE Trans. Haptics* **13**, 511–521 (2020).
24. AliAbbasi, E., Sormoli, M. R. A. & Basdogan, C. Frequency-Dependent Behavior of Electrostatic Forces Between Human Finger and Touch Screen Under Electroadhesion. *IEEE Trans. Haptics* **15**, 416–428 (2022).
25. Chen, R., Huang, Y. & Tang, Q. An analytical model for electrostatic adhesive dynamics on dielectric substrates. *J. Adhes. Sci. Technol.* **31**, 1229–1250 (2017).
26. Cao, C. et al. Theoretical model and design of electroadhesive pad with interdigitated electrodes. *Mater. Des.* **89**, 485–491 (2016).
27. Woo, S. J. & Higuchi, T. Electric field and force modeling for electrostatic levitation of lossy dielectric plates. *J. Appl. Phys.* **108**, 104906 (2010).
28. Qin, S. & McTeer, A. Wafer dependence of Johnsen–Rahbek type electrostatic chuck for semiconductor processes. *J. Appl. Phys.* **102**, 064901 (2007).
29. Guo, J. et al. Investigation of relationship between interfacial electroadhesive force and surface texture. *J. Phys. Appl. Phys.* **49**, 035303 (2015).
30. Bigharaz, M., Schenkel, T. & Bingham, P. A. Increasing force generation in electroadhesive devices through modelling of novel electrode geometries. *J. Electrostat.* **109**, 103540 (2021).
31. Stuckes, A. D. Some theoretical and practical considerations of the Johnsen–Rahbek effect. *Proc. IEE - Part B Radio Electron. Eng.* **103**, 125–131 (1956).
32. Koh, K. H., Sreekumar, M. & Ponnambalam, S. G. Experimental Investigation of the Effect of the Driving Voltage of an Electroadhesion Actuator. *Materials* **7**, 4963–4981 (2014).
33. Atkinson, R. A simple theory of the Johnsen–Rahbek effect. *J. Phys. Appl. Phys.* **2**, 325 (1969).
34. Krape, R. P. *Applications Study of Electroadhesive Devices*. <https://ntrs.nasa.gov/api/citations/19680028434/downloads/19680028434.pdf> (1968).
35. Ciavarella, M. & Papangelo, A. A Simplified Theory of Electroadhesion for Rough Interfaces. *Front. Mech. Eng.* **6**, 27 (2020).
36. Persson, B. N. J. & Guo, J. Electroadhesion for soft adhesive pads and robotics: theory and numerical results. *Soft Matter* **15**, 8032–8039 (2019).
37. Ruffatto, D., Parness, A. & Spenko, M. Improving controllable adhesion on both rough and smooth surfaces with a hybrid electrostatic/gecko-like adhesive. *J. R. Soc. Interface* **11**, 20131089 (2014).
38. Choi, K. et al. Lifting-Force Maximization of a Micropatterned Electroadhesive Device Comparable to the Human-Finger Grip. *ACS Appl. Electron. Mater.* **2**, 1596–1602 (2020).
39. Fundamental study of an electrostatic chuck for silicon wafer handling IEEE Journals & Magazine | IEEE Xplore. <https://ieeexplore-ieee-org.remotexs.ntu.edu.sg/abstract/document/1003438>.
40. Téllez, J. P. D., Krahn, J. & Menon, C. Characterization of electro-adhesives for robotic applications. In *2011 IEEE International Conference on Robotics and Biomimetics* 1867–1872 (2011). <https://doi.org/10.1109/ROBIO.2011.6181562>.
41. Guo, J. et al. Geometric Optimisation of Electroadhesive Actuators Based on 3D Electrostatic Simulation and its Experimental Verification. *IFAC-Pap* **49**, 309–315 (2016).
42. Kim, J.-H., Kang, S.-H. & Cho, S. Shape design optimization of interdigitated electrodes for maximal electro-adhesion forces. *Struct. Multidiscip. Optim.* **61**, 1843–1855 (2020).
43. Lai, S., Zhang, J., Yan, Y. & Yu, H. Optimization Design Strategy of Electroadhesive Devices with Interdigital Electrodes Based on the Multiparameters Theoretical Model. *Math. Probl. Eng.* **2021**, 3737490 (2021).
44. Ruffatto, D., Shah, J. & Spenko, M. Optimization and experimental validation of electrostatic adhesive geometry. In *2013 IEEE Aerospace Conference* 1–8 (2013). <https://doi.org/10.1109/AERO.2013.6496943>.
45. Li, X. et al. Electrowetting: A Consideration in Electroadhesion. *IEEE Trans. Haptics* **13**, 522–529 (2020).
46. Ayyildiz, M., Scaraggi, M., Sirin, O., Basdogan, C. & Persson, B. N. J. Contact mechanics between the human finger and a touchscreen under electroadhesion. *Proc. Natl. Acad. Sci.* **115**, 12668–12673 (2018).
47. Li, X. et al. Nanotexture Shape and Surface Energy Impact on Electroadhesive Human–Machine Interface Performance. *Adv. Mater.* **33**, 2008337 (2021).
48. AliAbbasi, E. et al. Effect of Finger Moisture on Tactile Perception of Electroadhesion. *IEEE Trans. Haptics* 1–9, <https://doi.org/10.1109/TOH.2024.3441670> (2024).
49. Savioli, L. et al. Morphing electroadhesive interface to manipulate uncooperative objects. In *Sensors and Smart Structures Technologies for Civil, Mechanical, and Aerospace Systems 2014* 9061 573–585 (SPIE, 2014).
50. Choi, C. et al. Effect of surface temperature on finger friction and perception in electroadhesion. In *2021 IEEE World Haptics Conference (WHC)* 680–684 (IEEE, 2021).
51. Hwang, G., Park, J., Cortes, D. S. D., Hyeon, K. & Kyung, K.-U. Electroadhesion-Based High-Payload Soft Gripper With Mechanically Strengthened Structure. *IEEE Trans. Ind. Electron.* **69**, 642–651 (2022).
52. Zhang, Y. et al. Thermal, Mechanical and Dielectric Properties of Polyimide Composite Films by In-Situ Reduction of Fluorinated Graphene. *Molecules* **27**, 8896 (2022).

53. Gu, G. Y., Zou, J., Zhao, R. K., Zhao, X. H. & Zhu, X. Y. Soft wall-climbing robots. *Sci. Robot.* **3**, eaat2874 (2018).
54. Guo, Y., Guo, J., Liu, L., Liu, Y. & Leng, J. Bioinspired multimodal soft robot driven by a single dielectric elastomer actuator and two flexible electroadhesive feet. *Extreme Mech. Lett.* **53**, 101720 (2022).
55. Xie, L., Wang, G., Jiang, C., Yu, F. & Zhao, X. Properties and Applications of Flexible Poly(Vinylidene Fluoride)-Based Piezoelectric Materials. *Crystals* **11**, 644 (2021).
56. Tiwari, V. & Srivastava, G. Effect of thermal processing conditions on the structure and dielectric properties of PVDF films. *J. Polym. Res.* **21**, 1–8 (2014).
57. Ranjithkumar, R. et al. Improved load bearing performance of electroadhesive tapes with Hexagonal boron nitride/Barium titanate composite in Poly (vinylidene fluoride co-hexafluoropropylene). *J. Mater. Sci. Mater. Electron.* **34**, 1–11 (2023).
58. Prahlad, H., Pelrine, R., Stanford, S., Marlow, J. & Kornbluh, R. Electroadhesive robots—wall climbing robots enabled by a novel, robust, and electrically controllable adhesion technology. In *2008 IEEE International Conference on Robotics and Automation* 3028–3033 (2008). <https://doi.org/10.1109/ROBOT.2008.4543670>.
59. Chen, R. et al. Bio-inspired shape-adaptive soft robotic grippers augmented with electroadhesion functionality. *Soft Robot* **6**, 701–712 (2019).
60. Romasanta, L. J., López-Manchado, M. A. & Verdejo, R. J. P. Increasing the performance of dielectric elastomer actuators: A review from the materials perspective. *Prog. Polym. Sci.* **51**, 188–211 (2015).
61. Ming Tan, M. W., Wang, H., Gao, D., Huang, P. & See Lee, P. Towards high performance and durable soft tactile actuators. *Chem. Soc. Rev.* **53**, 3485–3535 (2024).
62. Xiang, C., Guo, J. & Rossiter, J. Soft-smart robotic end effectors with sensing, actuation, and gripping capabilities. *Smart Mater. Struct.* **28**, 055034 (2019).
63. Kanno, R., Nagai, T. & Shintake, J. Rapid Fabrication Method for Soft Devices Using Off-the-Shelf Conductive and Dielectric Acrylic Elastomers. *Adv. Intell. Syst.* **3**, 2000173 (2021).
64. Choi, K. et al. Capturing Polar and Nonpolar Particles with an Electroadhesive Device Using Interfacial and Orientational Polarization. *ACS Sustain. Chem. Eng.* **9**, 13367–13375 (2021).
65. Gao, D. et al. A supramolecular gel-elastomer system for soft iontronic adhesives. *Nat. Commun.* **14**, 1990 (2023).
66. Park, S. et al. Stretchable and Soft Electroadhesion Using Liquid-Metal Subsurface Microelectrodes. *Adv. Mater. Technol.* **6**, 2100263 (2021).
67. Kim, S. et al. Stretchable and soft electroadhesion and capacitive sensors enabled by spider web-inspired interdigitated liquid metal subsurface microwires. *Chem. Eng. J.* **456**, 141018 (2023).
68. Duduta, M., Wood, R. J. & Clarke, D. R. Flexible, stretchable electroadhesives based on acrylic elastomers. In *Electroactive Polymer Actuators and Devices (EAPAD) 2016* 9798 234–241 (SPIE, 2016).
69. Wang, N., Cui, C., Chen, B. & Zhang, X. A Soft Gripper Based on Dielectric Elastomer Actuator. in *2017 IEEE 7th Annual International Conference on CYBER Technology in Automation, Control, and Intelligent Systems (CYBER)* 586–591 (2017). <https://doi.org/10.1109/CYBER.2017.8446451>.
70. Cacucciolo, V., Shea, H. & Carbone, G. Peeling in electroadhesion soft grippers. *Extreme Mech. Lett.* **50**, 101529 (2022).
71. Okuno, Y., Shigemune, H., Kuwajima, Y. & Maeda, S. Stretchable Suction Cup with Electroadhesion. *Adv. Mater. Technol.* **4**, 1800304 (2019).
72. Gao, X., Cao, C., Guo, J. & Conn, A. Elastic Electroadhesion with Rapid Release by Integrated Resonant Vibration. *Adv. Mater. Technol.* **4**, 1800378 (2019).
73. An, S. et al. Design and development of a variable structure gripper with electroadhesion. *Smart Mater. Struct.* **33**, 055035 (2024).
74. Mastrangelo, M., Caruso, F., Carbone, G. & Cacucciolo, V. Electroadhesion zipping with soft grippers on curved objects. *Extreme Mech. Lett.* **61**, 101999 (2023).
75. Minaminosono, A., Toyoda, R., Hosoya, N. & Maeda, S. Fabrication of a stretchable electroadhesive pad. In *2022 International Symposium on Micro-NanoMechatronics and Human Science (MHS)* 1–4 (2022). <https://doi.org/10.1109/MHS56725.2022.10092034>.
76. Goh, G. L., Zhang, H., Chong, T. H. & Yeong, W. Y. 3D Printing of Multilayered and Multimaterial Electronics: A Review. *Adv. Electron. Mater.* **7**, 2100445 (2021).
77. Martin, C. et al. A Review of Advanced Roll-to-Roll Manufacturing: System Modeling and Control. *J. Manuf. Sci. Eng.* **147**, 041004 (2024).
78. Testoni, O., Bodkhe, S., Ermanni, P. & Bergamini, A. Mechanical Characterization of a Novel Concept of Adaptive Electrostatic Friction Damper. In *Smart Materials, Adaptive Structures and Intelligent Systems* 84027 V001T01A013 (American Society of Mechanical Engineers, 2020).
79. Testoni, O., Bergamini, A., Bodkhe, S. & Ermanni, P. A novel concept for adaptive friction damper based on electrostatic adhesion. *Smart Mater. Struct.* **29**, 105032 (2020).
80. Feizi, N., Atashzar, S. F., Kermani, M. R. & Patel, R. V. Design and Modeling of a Smart Torque-Adjustable Rotary Electroadhesive Clutch for Application in Human–Robot Interaction. *IEEEASME Trans. Mechatron.* **28**, 2738–2748 (2023).
81. Diller, S. B., Collins, S. H. & Majidi, C. The effects of electroadhesive clutch design parameters on performance characteristics. *J. Intell. Mater. Syst. Struct.* **29**, 3804–3828 (2018).
82. Detailleur, A., Umans, S., Van Even, H., Pennycott, A. & Vallery, H. Feasibility Analysis of a Self-Reinforcing Electroadhesive Rotational Clutch. In *2021 IEEE/ASME International Conference on Advanced Intelligent Mechatronics (AIM)* 478–483 (2021). <https://doi.org/10.1109/AIM46487.2021.9517370>.
83. Amish, T. E., Auletta, J. T., Kessens, C. C., Smith, J. R. & Lipton, J. I. Johnsen-Rahbek Capstan Clutch: A High Torque Electrostatic Clutch. In *2024 IEEE International Conference on Robotics and Automation (ICRA)* 148–154 (2024). <https://doi.org/10.1109/ICRA57147.2024.10611283>.
84. Ramachandran, V., Shintake, J. & Floreano, D. All-Fabric Wearable Electroadhesive Clutch. *Adv. Mater. Technol.* **4**, 1800313 (2019).
85. Levine, D. J. et al. A Low-Voltage, High-Force Capacity Electroadhesive Clutch Based on Ionoelastomer Heterojunctions. *Adv. Mater.* **35**, 2304455 (2023).
86. West, J. D., Mici, J., Jaquith, J. F. & Lipson, H. Design and optimization of millimeter-scale electroadhesive grippers. *J. Phys. Appl. Phys.* **53**, 435302 (2020).
87. Guo, J., Xiang, C., Zanini, P. & Rossiter, J. Magnetic Augmented Self-sensing Flexible Electroadhesive Grippers. *IEEE Robot. Autom. Lett.* **4**, 2364–2369 (2019).
88. Cacucciolo, V., Shintake, J. & Shea, H. Delicate yet strong: Characterizing the electro-adhesion lifting force with a soft gripper. In *2019 2nd IEEE International Conference on Soft Robotics (RoboSoft)* 108–113 (2019). <https://doi.org/10.1109/ROBOSOFT.2019.8722706>.
89. Chen, R. et al. Variable Stiffness Electroadhesion and Compliant Electroadhesive Grippers. *Soft Robot* **9**, 1074–1082 (2022).
90. Vasudev, A. & Zhe, J. A low voltage capillary microgripper using electrowetting. In *TRANSDUCERS 2009 - 2009 International Solid-State Sensors, Actuators and Microsystems Conference* 825–828 (2009). <https://doi.org/10.1109/SENSOR.2009.5285747>.
91. De Rivaz, S. D. et al. Inverted and vertical climbing of a quadrupedal microrobot using electroadhesion. *Sci. Robot.* **3**, eaau3038 (2018).



92. Chatterjee, S. et al. Preferential Contamination in Electrodeposited Touchscreens: Mechanisms, Multiphysics Model, and Solutions. *Adv. Mater. Technol.* **8**, 2300213 (2023).
93. Park, B. et al. Flexible and Transparent Electrodeposition-Based Haptic Display with Low Driving Voltage. *ACS Appl. Mater. Interfaces* **16**, 55864–55872 (2024).
94. Zhang, K. & Follmer, S. Electrostatic adhesive brakes for high spatial resolution refreshable 2.5D tactile shape displays. In *2018 IEEE Haptics Symposium (HAPTICS)* 319–326 (2018). <https://doi.org/10.1109/HAPTICS.2018.8357195>.
95. Kawamoto, H. & Shibata, T. Electrostatic cleaning system for removal of sand from solar panels. *J. Electrostat.* **73**, 65–70 (2015).
96. Jaworek, A., Krupa, A. & Czech, T. Modern electrostatic devices and methods for exhaust gas cleaning: A brief review. *J. Electrostat.* **65**, 133–155 (2007).
97. Alizadehyazdi, V., Modabberifar, M., Mahmoudzadeh Akherat, S. M. J. & Spenko, M. Electrostatic self-cleaning gecko-like adhesives. *J. R. Soc. Interface* **15**, 20170714 (2018).
98. Branz, F. et al. Soft docking system for capture of irregularly shaped, uncontrolled space objects. *6th European Conference on Space Debris, ESA/ESOC, Darmstadt, Germany* (2013).
99. Beasley, G. & Hankins, W. Development of electrodeposited devices for zero-g intra/extravehicular activities. In *Weightlessness and Artificial Gravity Meeting* (American Institute of Aeronautics and Astronautics). <https://doi.org/10.2514/6.1971-853>.
100. Bryan, T., Macleod, T., Gagliano, L., Williams, S. & McCoy, B. Innovative Electrostatic Adhesion Technologies. In (Maui, HI, 2015).
101. Saravia, W. & Udrea, B. Highly compliant active clinging mechanism. In *2016 IEEE Aerospace Conference* 1–9 (2016). <https://doi.org/10.1109/AERO.2016.7500742>.
102. Leung, B. C., Goesser, N. R., Miller, L. A. & Gonzalez, S. Validation of electrodeposition as a docking method for spacecraft and satellite servicing. In *2015 IEEE Aerospace Conference* 1–8 (2015). <https://doi.org/10.1109/AERO.2015.7119283>.
103. Ritter, M. & Barnhart, D. Geometry characterization of electrodeposition samples for spacecraft docking application. In *2017 IEEE Aerospace Conference* 1–8 (2017). <https://doi.org/10.1109/AERO.2017.7943683>.
104. Levine, D. J., Turner, K. T. & Pikul, J. H. Materials with Electroprogrammable Stiffness. *Adv. Mater.* **33**, 2007952 (2021).
105. Xiang, C., Li, Z., Wang, F., Guan, Y. & Zhou, W. A 3D printed flexible electrodeposition gripper. *Sens. Actuators Phys.* **363**, 114675 (2023).
106. Shi, Y. et al. A processable, high-performance dielectric elastomer and multilayering process. *Science* **377**, 228–232 (2022).
107. Qiu, Y., Zhang, E., Plamthottam, R. & Pei, Q. Dielectric Elastomer Artificial Muscle: Materials Innovations and Device Explorations. *Acc. Chem. Res.* **52**, 316–325 (2019).
108. Tan, M. W. M., Thangavel, G. & Lee, P. S. Enhancing dynamic actuation performance of dielectric elastomer actuators by tuning viscoelastic effects with polar crosslinking. *NPG Asia Mater.* **11**, 62 (2019).
109. Wang, H. et al. A highly stretchable, self-healable, transparent and solid-state poly(ionic liquid) filler for high-performance dielectric elastomer actuators. *J. Mater. Chem. A* **11**, 14159–14168 (2023).
110. Tan, M. W. M., Bark, H., Thangavel, G., Gong, X. & Lee, P. S. Photothermal modulated dielectric elastomer actuator for resilient soft robots. *Nat. Commun.* **13**, 6769 (2022).
111. Molberg, M. et al. High Breakdown Field Dielectric Elastomer Actuators Using Encapsulated Polyaniline as High Dielectric Constant Filler. *Adv. Funct. Mater.* **20**, 3280–3291 (2010).
112. Sung Seo, J. et al. Nano-Sized rGO-Encapsulated TiO<sub>2</sub> Nanowire-Filled PDMS cone type dielectric elastomer actuator operating at low applied electric field. *Chem. Eng. J.* **494**, 152801 (2024).
113. Guo, J., Xiang, C. & Rossiter, J. A soft and shape-adaptive electrodeposited composite gripper with proprioceptive and exteroceptive capabilities. *Mater. Des.* **156**, 586–587 (2018).
114. Xiang, C., Guan, Y., Zhu, H., Lin, S. & Song, Y. All 3D printed ready-to-use flexible electrodeposition pads. *Sens. Actuators Phys.* **344**, 113747 (2022).
115. Skylar-Scott, M. A., Mueller, J., Visser, C. W. & Lewis, J. A. Voxellated soft matter via multimaterial multi-nozzle 3D printing. *Nature* **575**, 330–335 (2019).
116. Zhang, Y.-F. et al. Fast-Response, Stiffness-Tunable Soft Actuator by Hybrid Multimaterial 3D Printing. *Adv. Funct. Mater.* **29**, 1806698 (2019).
117. Xin, Y., Zhou, X., Bark, H. & Lee, P. S. The Role of 3D Printing Technologies in Soft Grippers. *Adv. Mater.* **36**, 2307963 (2024).
118. Huang, P., Fu, H., Tan, M. W. M., Jiang, Y. & Lee, P. S. Digital Light Processing 3D-Printed Multilayer Dielectric Elastomer Actuator for Vibrotactile Device. *Adv. Mater. Technol.* **9**, 2301642 (2024).
119. Tawk, C. & Alici, G. A Review of 3D-Printable Soft Pneumatic Actuators and Sensors: Research Challenges and Opportunities. *Adv. Intell. Syst.* **3**, 2000223 (2021).
120. Chortos, A., Hajiesmaili, E., Morales, J., Clarke, D. R. & Lewis, J. A. 3D Printing of Interdigitated Dielectric Elastomer Actuators. *Adv. Funct. Mater.* **30**, 1907375 (2020).
121. Demir, K. G., Zhang, Z., Yang, J. & Gu, G. X. Computational and Experimental Design Exploration of 3D-Printed Soft Pneumatic Actuators. *Adv. Intell. Syst.* **2**, 2000013 (2020).
122. Zolfagharian, A. et al. 3D/4D-printed bending-type soft pneumatic actuators: fabrication, modelling, and control. *Virtual Phys. Prototyp.* **15**, 373–402 (2020).
123. Gunawardane, P. D. S. H. et al. A Versatile 3D-Printable Soft Pneumatic Actuator Design for Multi-Functional Applications in Soft Robotics. *Soft Robot* **11**, 709–723 (2024).
124. Kim, H. J. et al. Low-Voltage Reversible Electrodeposition of Ionomer Junctions. *Adv. Mater.* **32**, 2000600 (2020).
125. Lu, S. et al. Reversible electrodeposition induced through low ion concentration migration for biomedical applications. *Chem. Eng. J.* **486**, 150393 (2024).
126. Bharti, S. Adhesives and adhesion technologies: a critical review. *Am. J. Polym. Sci. Technol.* **4**, 36 (2018).
127. Marques, A. C. et al. Review on Adhesives and Surface Treatments for Structural Applications: Recent Developments on Sustainability and Implementation for Metal and Composite Substrates. *Materials* **13**, 5590 (2020).
128. Chen, R., Wu, L., Sun, Y., Chen, J.-Q. & Guo, J.-L. Variable stiffness soft pneumatic grippers augmented with active vacuum adhesion. *Smart Mater. Struct.* **29**, 105028 (2020).
129. Song, S., Drotlef, D.-M., Son, D., Koivikko, A. & Sitti, M. Adaptive Self-Sealing Suction-Based Soft Robotic Gripper. *Adv. Sci.* **8**, 2100641 (2021).
130. Mantriota, G. Optimal grasp of vacuum grippers with multiple suction cups. *Mech. Mach. Theory* **42**, 18–33 (2007).
131. Tavakoli, M., Lourenço, J., Viegas, C., Neto, P. & de Almeida, A. T. The hybrid OmniClimber robot: Wheel based climbing, arm based plane transition, and switchable magnet adhesion. *Mechatronics* **36**, 136–146 (2016).
132. Gao, X., Yan, L., Wang, G. & Chen, I.-M. Modeling and Analysis of Magnetic Adhesion Module for Wall-Climbing Robot. *IEEE Trans. Instrum. Meas.* **72**, 1–9 (2023).
133. Wang, W., Liu, Y. & Xie, Z. Gecko-Like Dry Adhesive Surfaces and Their Applications: A Review. *J. Bionic Eng.* **18**, 1011–1044 (2021).
134. Liu, L., Li, L., Zhang, S., Xu, W. & Wang, Q. Polyimide-Based Dielectric Materials for High-Temperature Capacitive Energy Storage. *Electron. Mater.* **5**, 303–320 (2024).
135. Wang, T. et al. Enhanced Thermal Conductivity of Polyimide Composites with Boron Nitride Nanosheets. *Sci. Rep.* **8**, 1–8 (2018).
136. Meng, S., Zhao, T., Wang, X., Wang, X. & Zhang, Y. High-dielectric PVDF/MXene composite dielectric materials for energy storage

- preparation and performance study. *Polym. Compos.* **45**, 3460–3473 (2024).
137. Vaicekauskaitė, J., Mazurek, P., Vudayagiri, S. & Skov, A. L. Mapping the mechanical and electrical properties of commercial silicone elastomer formulations for stretchable transducers. *J. Mater. Chem. C* **8**, 1273–1279 (2020).
138. Atiqah, A., Mastura, M. T., Ali, B. A. A., Jawaid, M. & Sapuan, S. M. A Review on Polyurethane and its Polymer Composites. *Curr. Org. Synth.* **14**, 233–248 (2017).
139. Choi, C. et al. High-Performance and High Bandwidth Electro-adhesive Clutch Enabled by Fracture Mechanics and a Dielectric Nanoparticle-Based High-k Composite. *Adv. Mater. Technol.* **9**, 2301949 (2024).
140. Wang, Y. et al. Folding for Stiffening: A Novel Corrugated Electro-Adhesive Clutch. In *2023 IEEE International Conference on Robotics and Biomimetics (ROBIO)* 1–6 (2023). <https://doi.org/10.1109/ROBIO58561.2023.10354573>.

## Acknowledgements

This work was supported by the National Research Foundation (NRF), Prime Minister's Office, Singapore, under the Campus of Research Excellence and Technological Enterprise program, Smart Grippers for Soft Robotics project (Grant No. SGSR CREATE), and Ministry of Education AcRF Tier 2 grant no. MOE-T2EP50122-0002.

## Author contributions

P.H. conceived the topic and led the literature review and manuscript preparation. P.H. and Y.X. jointly conducted the analysis, prepared figures, and wrote the manuscript. P.S.L. supervised the work and provided critical revisions. All authors read and approved the final manuscript.

## Competing interests

The authors declare no competing interests.

## Additional information

**Correspondence** and requests for materials should be addressed to Pooi See Lee.

**Reprints and permissions information** is available at <http://www.nature.com/reprints>

**Publisher's note** Springer Nature remains neutral with regard to jurisdictional claims in published maps and institutional affiliations.

**Open Access** This article is licensed under a Creative Commons Attribution-NonCommercial-NoDerivatives 4.0 International License, which permits any non-commercial use, sharing, distribution and reproduction in any medium or format, as long as you give appropriate credit to the original author(s) and the source, provide a link to the Creative Commons licence, and indicate if you modified the licensed material. You do not have permission under this licence to share adapted material derived from this article or parts of it. The images or other third party material in this article are included in the article's Creative Commons licence, unless indicated otherwise in a credit line to the material. If material is not included in the article's Creative Commons licence and your intended use is not permitted by statutory regulation or exceeds the permitted use, you will need to obtain permission directly from the copyright holder. To view a copy of this licence, visit <http://creativecommons.org/licenses/by-nc-nd/4.0/>.

© The Author(s) 2025